



HAL
open science

Finite element analysis of a spectral problem on curved meshes occurring in diffusion with high order boundary conditions

Fabien Caubet, Joyce Ghantous, Charles Pierre

► To cite this version:

Fabien Caubet, Joyce Ghantous, Charles Pierre. Finite element analysis of a spectral problem on curved meshes occurring in diffusion with high order boundary conditions. 2024. hal-04552691

HAL Id: hal-04552691

<https://hal.science/hal-04552691>

Preprint submitted on 19 Apr 2024

HAL is a multi-disciplinary open access archive for the deposit and dissemination of scientific research documents, whether they are published or not. The documents may come from teaching and research institutions in France or abroad, or from public or private research centers.

L'archive ouverte pluridisciplinaire **HAL**, est destinée au dépôt et à la diffusion de documents scientifiques de niveau recherche, publiés ou non, émanant des établissements d'enseignement et de recherche français ou étrangers, des laboratoires publics ou privés.

Finite element analysis of a spectral problem on curved meshes occurring in diffusion with high order boundary conditions

Fabien Caubet*, Joyce Ghantous*, Charles Pierre*

April 18, 2024

Abstract

In this work is considered a spectral problem, involving a second order term on the domain boundary: the Laplace-Beltrami operator. A variational formulation is presented, leading to a finite element discretization. For the Laplace-Beltrami operator to make sense on the boundary, the domain is smooth: consequently the computational domain (classically a polygonal domain) will not match the physical one. Thus, the physical domain is discretized using high order curved meshes so as to reduce the *geometric error*. The *lift operator*, which is aimed to transform a function defined on the mesh domain into a function defined on the physical one, is recalled. This *lift* is a key ingredient in estimating errors on eigenvalues and eigenfunctions. A bootstrap method is used to prove the error estimates, which are expressed both in terms of *finite element approximation error* and of *geometric error*, respectively associated to the finite element degree $k \geq 1$ and to the mesh order $r \geq 1$. Numerical experiments are led on various smooth domains in 2D and 3D, which allow us to validate the presented theoretical results.

Key words: Laplace-Beltrami operator, A priori error estimates, Ventcel boundary conditions, Spectral problem, Finite element analysis, Curved mesh, Geometric error.

AMS subject classification: 65G99; 65N25; 65N15; 65N30; 35B45.

1 Introduction

Motivation ad objective. This work is part of a research program on the study of vibrating properties of mechanical parts submitted to intense and varying rotating regimes, more specifically when these parts are surrounded by thin surface layers (either specific industrial treatments or corrosion) that may impact or alter their mechanical properties. The general objective is to use shape optimization to better understand such mechanical parts and improve their design. This work is part of the RODAM research project¹.

From the numerical point of view, taking into account thin layers around mechanical parts induces specific difficulties, in particular when discretizing the domain with a mesh size adapted to the thin layer. To overcome this issue, the thin layer is modeled by adapted boundary conditions involving second order terms such as the Laplace-Beltrami operator. These conditions derive from

*Université de Pau et des Pays de l'Adour, E2S UPPA, CNRS, LMAP, UMR 5142, 64000 Pau, France. fabien.caubet@univ-pau.fr, joyce.ghantous@univ-pau.fr, charles.pierre@univ-pau.fr

¹*Robust Optimal Design under Additive Manufacturing constraints:* <https://lma-umr5142.univ-pau.fr/en/scientific-activities/scientific-challenges/rodam.html>

the pioneering works of Ventcel in [33, 34]. For the second order boundary terms to make sense, the domain is assumed to be smooth. Thus, we have to deal with problems where the physical domain and the mesh domain differ, putting forward an intrinsic geometric error.

Towards this general objective of optimizing spectral properties for the elastic behavior of mechanical parts surrounded by specific thin layers, the present paper addresses the numerical resolution of the direct problem. The original problem is first simplified considering in a first step a scalar diffusion problem instead of the vector linear elasticity framework. Our aim is to analyze the numerical errors when solving the spectral problems both when considering the error induced by the numerical method and the geometric error caused when discretizing the domain.

This paper thus is devoted to the numerical analysis of a spectral elliptic problem equipped with a non classical boundary condition involving a high order tangential operator, here the Laplace-Beltrami operator: the so-called *Ventcel boundary condition* (we refer, e.g., to [25] for a general derivation of these boundary conditions).

The Ventcel eigenvalue problem. Let Ω be a nonempty bounded connected smooth domain of \mathbb{R}^d , $d = 2, 3$, with a smooth boundary $\Gamma := \partial\Omega$. Motivated by generalized impedance boundary conditions, we consider the following spectral problem with Ventcel boundary conditions,

$$\begin{cases} -\Delta u = \lambda u & \text{in } \Omega, \\ -\Delta_\Gamma u + \partial_n u + u = 0 & \text{on } \Gamma, \end{cases} \quad (1.1)$$

where $\partial_n u$ is the normal derivative of u along Γ and Δ_Γ the Laplace-Beltrami operator (see below for a reminder of the definition). The operator associated to this problem is a self-adjoint positive-definite operator. Consequently, the spectrum of Problem (1.1) consists of an increasing sequence of positive eigenvalues tending to infinity. For each eigenvalue there exists a finite number of associated eigenfunctions defined on Ω . In [27], the authors delivered a thorough study of the well-posedness of the Ventcel problem with source terms and the regularity of its solution.

As previously mentioned, the domain Ω is required to be smooth due to the presence of second order boundary conditions. Therefore the physical domain Ω cannot match the mesh domain Ω_h inducing an intrinsic geometric error. This error is larger when using classical affine meshes made of triangles in 2D and tetrahedrals in 3D. Indeed, these polygonal meshes will induce a saturation of the numerical error at a low order: when resorting to accurate finite element methods the geometric error will dominate. To improve the error rate, we will resort to curved meshes whose elements have polynomial degree $r \geq 1$ so as to have a geometric error with a better asymptotic regime with respect to the mesh size.

A technical difficulty arises: the mesh domain of order r , denoted $\Omega_h^{(r)}$, does not fit exactly on Ω . A \mathbb{P}^k -Lagrangian finite element method is used with a degree $k \geq 1$ to approximate the exact solutions of System (1.1). In order to estimate the error between the discrete eigenfunctions defined on $\Omega_h^{(r)}$ and the exact ones defined on Ω , a *lift operator* is required. Throughout the years, many authors defined their version of the *lift functional*, like in [16, 29, 30, 14, 15, 17]. Among them, Dubois defined a lift based on the orthogonal projection onto the domain boundary Γ in [16]. The idea of relying on the orthogonal projection in the lift definition was reintroduced by Dzuik in [17] in order to define a surface lift. This was generalised in the case of *lifting* a function from higher order surface meshes onto a continuous surface in [14] by Demlow. In the context of curved meshes with order $r \geq 2$, the definition of a volume lift required a higher regularity: such an improvement was brought by Elliott *et al.* in [20], with a definition that also relies on the orthogonal projection. However, their definition of the volume lift did not fit the orthogonal projection on the computational domain's boundary, as we highlighted in [9]. It is natural to

expect the volume lift to fit the orthogonal projection on the mesh boundary: such a property is crucial for the derivation of *a priori* error estimates in [9] and in the present paper. Thus, we recently formulated an alternative definition of a volume lift in [9] to satisfy that property together with all the necessary regularity properties, which will be adopted and recalled in this paper.

State of the art and main results. In 2013, Elliott and Ranner in [20] made a numerical analysis of a bulk problem with a Ventcel boundary condition on curved meshes with iso-parametric finite elements. More recently the approximation of the Ventcel problem with source terms has been studied in [19, 9] with curved meshes and high order finite elements. In [20, 19], the same lift definition was considered fulfilling its role in enabling the authors to estimate the error on a smooth domain while using an isoparametric approach. In [9, 10], a non isoparametric approach is led while distinguishing between the mesh order r and the degree of the finite element method k , using a different definition of the lift operator as previously discussed. This lift definition is considered in this work and recalled in Section 3.

Meanwhile, in 2018, error estimates for spectral problem on curved meshes have been carried out in [6] by Bonito *et al.* for the surface Laplacian. The ideas of [6] are adapted and extended in the present paper in the case of a volume spectral problem. The main novelties is the use of the new lift operator defined in [9] to estimate the eigenvalue and eigenfunction error both in terms of finite element approximation error and of geometric error, respectively, associated to the finite element degree $k \geq 1$ and to the mesh order $r \geq 1$. To the authors' knowledge, no error analysis was made on a bulk spectral problem having Ventcel type conditions. Let us also emphasize that the theoretical study and the numerical resolution of this spectral problem involve non-trivial difficulties compared with the analysis of the direct problem we made in [9].

The main result of this paper can be summarized as follows (see Theorem 5.1 for a precise statement). Let λ_i be an eigenvalue of multiplicity N with its corresponding eigenfunctions, $\{u_j\}_{j \in J}$, where $J := \{i, \dots, i + N - 1\}$, relatively to Problem (1.1). Then, there exists a mesh independent constant $c_{\lambda_i} > 0$, such that, for any $j \in J$,

$$\begin{aligned} |\lambda_j - \Lambda_j| &\leq c_{\lambda_i} (h^{2k} + h^{r+1}), \\ \inf_{U \in \mathbb{F}_h^\ell} \|u_j - U\|_{L^2(\Omega)} &\leq c_{\lambda_i} (h^{k+1} + h^{r+1/2}), \\ \inf_{U \in \mathbb{F}_h^\ell} \|u_j - U\|_{H^1(\Omega, \Gamma)} &\leq c_{\lambda_i} (h^k + h^{r+1/2}), \end{aligned}$$

where Λ_j is the eigenvalue of the discretization of (1.1) of rank $j \in J$, \mathbb{F}_h is the space generated by the discrete eigenfunctions associated to $\{\Lambda_j\}_{j \in J}$, \mathbb{F}_h^ℓ is the lift of \mathbb{F}_h made of functions defined on the physical domain Ω and where h is the mesh size. The Hilbert spaces $H^1(\Omega, \Gamma)$, precisely defined below, is made of the functions in $H^1(\Omega)$ having their traces in $H^1(\Gamma)$.

A *bootstrap method* is used to prove these error estimates. To sum up the main ideas of the proof, a preliminary estimation of the eigenvalue error is needed in order to estimate the eigenfunction error in the $L^2(\Omega)$ and $H^1(\Omega, \Gamma)$ norms using orthogonal projections over the space \mathbb{F}_h^ℓ . Lastly, we are able to obtain the adequate eigenvalue error estimate with respect to the finite element degree k and the geometric order of the mesh r using the obtained estimates on the eigenfunctions.

We validate these estimations in several numerical experiments presented in two and three dimensions. We noticed a *super-convergence* of the error rate on the quadratic meshes, which is much better than expected, as it was also depicted in [6]. In an attempt to understand the origin of this phenomena, numerical experiments are led on a non-symmetric, non convex domain and also on classical domains like the unit disk and the unit ball. However, the same asymptotic regime of the errors is observed on these various smooth domains.

Paper organization. Section 2 contains all the mathematical tools and useful definitions to derive the weak formulation of System (1.1). Section 3 is devoted to the definition of the high order meshes and the lift operator with some of its most essential properties. A Lagrangian finite element space and a discrete formulation of System (1.1) are presented in Section 4, alongside their *lifted forms* onto Ω . In Section 5 is stated the main result and are detailed the proofs of the eigenvalue and eigenfunction estimates. The paper wraps up in Section 6 with numerical experiments studying the convergence rates of the eigenvalue and eigenfunction errors over various domains in 2D and 3D.

2 The continuous problem

Needed mathematical tools. Firstly, let us introduce the notations that we adopt in this paper. Throughout this paper, Ω is a nonempty bounded connected open subset of \mathbb{R}^d ($d = 2, 3$) with a smooth (at least \mathcal{C}^2) boundary $\Gamma := \partial\Omega$. The unit normal to Γ pointing outwards is denoted by \mathbf{n} and $\partial_n u$ is the normal derivative of a function u . We denote respectively by $L^2(\Omega)$ and $L^2(\Gamma)$ the usual Lebesgue spaces endowed with their standard norms on Ω and Γ . Moreover, for $k \geq 1$, $H^k(\Omega)$ denotes the usual Sobolev space endowed with its standard norm. We also consider the Sobolev spaces $H^k(\Gamma)$ on the boundary as defined e.g. in [27, §2.3]. It is recalled that the norm on $H^1(\Gamma)$ is : $\|u\|_{H^1(\Gamma)}^2 := \|u\|_{L^2(\Gamma)}^2 + \|\nabla_\Gamma u\|_{L^2(\Gamma)}^2$, where ∇_Γ is the tangential gradient defined below; and that $\|u\|_{H^k(\Gamma)}^2 := \|u\|_{H^{k-1}(\Gamma)}^2 + \|\nabla_\Gamma u\|_{H^{k-1}(\Gamma)}^2$. Throughout this work, we rely on the following Hilbert space (see [27])

$$H^1(\Omega, \Gamma) := \{u \in H^1(\Omega), u|_\Gamma \in H^1(\Gamma)\},$$

equipped with the norm $\|u\|_{H^1(\Omega, \Gamma)}^2 := \|u\|_{H^1(\Omega)}^2 + \|u\|_{H^1(\Gamma)}^2$. In a similar way is defined the following space $L^2(\Omega, \Gamma) := \{u \in L^2(\Omega), u|_\Gamma \in L^2(\Gamma)\}$, equipped with the norm $\|u\|_{L^2(\Omega, \Gamma)}^2 := \|u\|_{L^2(\Omega)}^2 + \|u\|_{L^2(\Gamma)}^2$. More generally, we define $H^k(\Omega, \Gamma) := \{u \in H^k(\Omega), u|_\Gamma \in H^k(\Gamma)\}$.

Secondly, to understand more the so-called Ventcel boundary conditions, we recall the definition of the Laplace-Beltrami operator (see [26]): the *Laplace-Beltrami* operator of $u \in H^2(\Gamma)$ is given by,

$$\Delta_\Gamma u := \operatorname{div}_\Gamma(\nabla_\Gamma u),$$

where,

- the *tangential gradient* of u is given by $\nabla_\Gamma u := \nabla \tilde{u} - (\nabla \tilde{u} \cdot \mathbf{n})\mathbf{n}$, with $\tilde{u} \in H^1(\mathbb{R}^d)$ being any extension of u ;
- the *tangential divergence* of $W \in H^1(\Gamma, \mathbb{R}^d)$ is $\operatorname{div}_\Gamma W := \operatorname{div} \tilde{W} - (D\tilde{W} \mathbf{n}) \cdot \mathbf{n}$, where $\tilde{W} \in H^1(\mathbb{R}^d, \mathbb{R}^d)$ is any extension of W and $D\tilde{W}$ is the differential of \tilde{W} ;

Finally, the construction of the mesh used in Section 3 is based on the following fundamental result that may be found in [13] and [24, §14.6]. For more details on the geometrical properties of the tubular neighborhood and the orthogonal projection defined below, we refer to [14, 15, 18].

Proposition 2.1. *Let Ω be a nonempty bounded connected open subset of \mathbb{R}^d ($d = 2, 3$) with a \mathcal{C}^2 boundary $\Gamma = \partial\Omega$. Let $d : \mathbb{R}^d \rightarrow \mathbb{R}$ be the signed distance function with respect to Γ defined by,*

$$d(x) := \begin{cases} -\operatorname{dist}(x, \Gamma) & \text{if } x \in \Omega, \\ 0 & \text{if } x \in \Gamma, \\ \operatorname{dist}(x, \Gamma) & \text{otherwise,} \end{cases} \quad \text{with } \operatorname{dist}(x, \Gamma) := \inf \{|x - y|, y \in \Gamma\}.$$

Then there exists a tubular neighborhood $\mathcal{U}_\Gamma := \{x \in \mathbb{R}^d; |d(x)| < \delta_\Gamma\}$ of Γ , of sufficiently small width δ_Γ , where d is a \mathcal{C}^2 function. Its gradient ∇d is an extension of the external unit normal \mathbf{n} to Γ . Additionally, in this neighborhood \mathcal{U}_Γ , the orthogonal projection b onto Γ is uniquely defined and given by,

$$b : x \in \mathcal{U}_\Gamma \longmapsto b(x) := x - d(x)\nabla d(x) \in \Gamma.$$

Well posedness of the spectral problem. Throughout the rest of the paper, dx and ds denote respectively the volume and surface measures on Ω and on Γ .

The variational formulation of the studied problem (1.1) is classically obtained, using the integration by parts formula on the surface Γ (see, e.g., [26]): it is then given by,

$$\begin{cases} \text{find } (\lambda, u) \in \mathbb{R} \times \mathbf{H}^1(\Omega, \Gamma), \text{ such that,} \\ a(u, v) = \lambda m(u, v), \quad \forall v \in \mathbf{H}^1(\Omega, \Gamma), \end{cases} \quad (2.1)$$

where a is the bilinear form, defined on $[\mathbf{H}^1(\Omega, \Gamma)]^2$, given by,

$$a(u, v) := \int_{\Omega} \nabla u \cdot \nabla v \, dx + \int_{\Gamma} \nabla_{\Gamma} u \cdot \nabla_{\Gamma} v \, ds + \int_{\Gamma} uv \, ds,$$

and m is the bilinear form, defined on $[\mathbf{H}^1(\Omega, \Gamma)]^2$, given by,

$$m(u, v) := \int_{\Omega} uv \, dx.$$

The bilinear form a , being symmetric and continuous, is also coercive with respect to the norm over $\mathbf{H}^1(\Omega, \Gamma)$, as proved in [10, Theorem 2]. The second bilinear form m is none other than the scalar product on the space $L^2(\Omega)$. Then by a classical spectral result (see [1, Theorem 7.3.2]), we claim the existence of an infinite number of eigenvalues to Problem (2.1), which form an increasing sequence $(\lambda_n)_{n \geq 1} \subset \mathbb{R}_+^*$ of positive real numbers, tending to infinity. Their associated eigenfunctions form an orthonormal Hilbert basis of $L^2(\Omega)$, denoted $(u_n)_{n \geq 1}$ satisfying,

$$u_n \in \mathbf{H}^1(\Omega, \Gamma), \quad a(u_n, v) = \lambda_n m(u_n, v), \quad \forall v \in \mathbf{H}^1(\Omega, \Gamma).$$

Assuming that the eigenvalues are counted with their multiplicity and ordered increasingly, the aim of this work is to approximate an eigenvalue λ_i of multiplicity $N \geq 1$ and its associated eigenfunctions $\{u_j\}_{j \in J}$, which are m -orthonormal, with $J = \{i, \dots, i + N - 1\}$ the set of indices (see [22, page 5]).

3 Curved mesh and lift definition

Throughout this section, we briefly explain the construction of curved meshes of geometrical order $r \geq 1$ of the domain Ω and give the main associated notations. We refer to Appendix A for details and rigorous definitions (in particular concerning the mentioned transformations). Additionally, the definition of the lift operator with some essential lift properties are recalled. We refer to [9, §3, §4] for more exhaustive details and properties. The set of polynomials in \mathbb{R}^d of order r or less is denoted by \mathbb{P}^r . From now on, the domain Ω , is assumed to be at least \mathcal{C}^{r+2} regular, and \hat{T} denotes the reference simplex of dimension d .

Let $\mathcal{T}_h^{(1)}$ be a polyhedral quasi-uniform mesh of Ω made of simplices of dimension d , denoted T (triangles or tetrahedra). The mesh domain $\Omega_h^{(1)} := \left\{ \cup T, T \in \mathcal{T}_h^{(1)} \right\}$ does not coincide with the physical domain Ω , which is smooth. Each mesh element T is the image of the reference simplex \hat{T}

by the affine transformation $F_T : \hat{T} \rightarrow T$. An exact mesh $\mathcal{T}_h^{(e)}$ (with domain Ω) is built. To each element $T \in \mathcal{T}_h^{(1)}$ is associated a transformation $F_T^{(e)} : \hat{T} \rightarrow T^{(e)} := F_T^{(e)}(\hat{T})$, which is defined with the help of F_T in Definition A.2. The elements of the exact mesh $\mathcal{T}_h^{(e)}$ exactly are $\left\{ T^{(e)} = F_T^{(e)}(\hat{T}), T \in \mathcal{T}_h^{(1)} \right\}$, where the exact elements $T^{(e)}$ share the same vertices as T . All the details are given in Appendix A.

Curved mesh $\mathcal{T}_h^{(r)}$ of order r . The exact mapping $F_T^{(e)}$, defined in Appendix A, is interpolated as a polynomial of order $r \geq 1$ in the classical \mathbb{P}^r -Lagrange basis on \hat{T} . The interpolant is denoted by $F_T^{(r)}$, which is a \mathcal{C}^1 -diffeomorphism and is in $\mathcal{C}^{r+1}(\hat{T})$ (see [11, chap. 4.3]). For more exhaustive details and properties of this transformation, we refer to [20, 12, 11]. Note that, by definition, $F_T^{(r)}$ and $F_T^{(e)}$ coincide on all \mathbb{P}^r -Lagrange nodes in \hat{T} . The curved mesh of order r is $\mathcal{T}_h^{(r)} := \left\{ T^{(r)} := F_T^{(r)}(\hat{T}); T \in \mathcal{T}_h^{(1)} \right\}$, $\Omega_h^{(r)} := \cup_{T^{(r)} \in \mathcal{T}_h^{(r)}} T^{(r)}$ is the mesh domain and $\Gamma_h^{(r)} := \partial\Omega_h^{(r)}$ is its boundary.

Functional lift. In order to lift a function from the mesh domain onto Ω , a well defined transformation going from $\Omega_h^{(r)}$ to Ω is needed. In a previous work [9], the transformation $G_h^{(r)}$ was defined piece-wise such that,

$$G_h^{(r)} : \Omega_h^{(r)} \rightarrow \Omega; \quad G_h^{(r)}|_{\Gamma_h^{(r)}} = b,$$

where b is the orthogonal projection defined in Proposition 2.1. We refer to Appendix B for the full expression of $G_h^{(r)}$.

By construction, $G_h^{(r)}$ is globally continuous and piecewise differentiable on each mesh element. Additionally, quoting [9, Proposition 2], where the full proof is detailed: let $T^{(r)} \in \mathcal{T}_h^{(r)}$, the mapping $G_h^{(r)}|_{T^{(r)}}$ is $\mathcal{C}^{r+1}(T^{(r)})$ regular and a \mathcal{C}^1 -diffeomorphism from $T^{(r)}$ onto $T^{(e)}$. Moreover, for a sufficiently small mesh size h , there exists a constant $c > 0$, independent of h , such that,

$$\forall x \in T^{(r)}, \quad \|DG_h^{(r)}(x) - \text{Id}\| \leq ch^r \quad \text{and} \quad |J_h(x) - 1| \leq ch^r. \quad (3.1)$$

where $DG_h^{(r)}$ is the differential of $G_h^{(r)}$ and J_h is its Jacobin.

Definition 3.1. To $u_h \in L^2(\Omega_h^{(r)}, \Gamma_h^{(r)})$ is associated its lift, denoted $u_h^\ell \in L^2(\Omega, \Gamma)$, given by,

$$u_h^\ell \circ G_h^{(r)} := u_h.$$

The lift satisfies the trace property which states

$$\forall u_h \in H^1(\Omega_h^{(r)}), \quad (\text{Tr } u_h)^\ell = \text{Tr}(u_h^\ell).$$

Remark 3.1. The above trace property is essential in the error analysis detailed in Section 5. This is due to the fact that the restriction of $G_h^{(r)}$ to $\Gamma_h^{(r)}$ is equal to the orthogonal projection: $G_h^{(r)}|_{\Gamma_h^{(r)}} = b$.

Lift properties. The results presented in this section can be found with more details in [14, 15, 9]. Consider $u_h, v_h \in H^1(\Omega_h)$ and let $u_h^\ell, v_h^\ell \in H^1(\Omega)$ be their respected lifts, we have,

$$\int_{\Omega_h} u_h v_h \, dx = \int_{\Omega} u_h^\ell v_h^\ell \frac{1}{J_h^\ell} \, dx, \quad (3.2)$$

where J_h denotes the Jacobian of $G_h^{(r)}$ and J_h^ℓ is its lift given by $J_h^\ell \circ G_h^{(r)} = J_h$.

Note that for any $x \in \Omega_h^{(r)}$, using a change of variables $z = G_h^{(r)}(x) \in \Omega$, one has, $(\nabla v_h)^\ell(z) = {}^\top \text{DG}_h^{(r)}(x) \nabla v_h^\ell(z)$, where ${}^\top \text{DG}_h^{(r)}$ is the transpose of $\text{DG}_h^{(r)}$. Introducing the notation, $\mathcal{G}_h^{(r)}(z) := {}^\top \text{DG}_h^{(r)}(x)$, one has,

$$\int_{\Omega_h^{(r)}} \nabla u_h \cdot \nabla v_h \, dx = \int_{\Omega} \mathcal{G}_h^{(r)}(\nabla u_h^\ell) \cdot \mathcal{G}_h^{(r)}(\nabla v_h^\ell) \frac{1}{J_h^\ell} \, dx. \quad (3.3)$$

A direct consequence of the inequalities (3.1), using the lift definition 3.1, is that both $\mathcal{G}_h^{(r)}$ and J_h^ℓ are bounded on $T^{(e)}$. Additionally, we have the following inequalities, which are a key ingredient for the proof of the error estimations,

$$\forall x \in T^{(e)}, \quad \|\mathcal{G}_h^{(r)}(x) - \text{Id}\| \leq ch^r \quad \text{and} \quad \left| \frac{1}{J_h^\ell(x)} - 1 \right| \leq ch^r. \quad (3.4)$$

Similarly, let $u_h, v_h \in H^1(\Gamma_h)$ with $u_h^\ell, v_h^\ell \in H^1(\Gamma)$ as their respected lifts. Then, one has,

$$\int_{\Gamma_h^{(r)}} u_h v_h \, ds = \int_{\Gamma} u_h^\ell v_h^\ell \frac{1}{J_b^\ell} \, ds, \quad (3.5)$$

where J_b denotes the Jacobian of the orthogonal projection b defined in Proposition 2.1, and J_b^ℓ is its lift given by $J_b^\ell \circ b = J_b$.

A similar equation can be written with tangential gradients, given by the following expression,

$$\int_{\Gamma_h^{(r)}} \nabla_{\Gamma_h^{(r)}} u_h \cdot \nabla_{\Gamma_h^{(r)}} v_h \, ds_h = \int_{\Gamma} A_h^\ell \nabla_{\Gamma} u_h^\ell \cdot \nabla_{\Gamma} v_h^\ell \, ds, \quad (3.6)$$

where A_h^ℓ is the lift of the matrix A_h defined in [9, 14].

We recall two important estimates proved in [14] relative to A_h and J_b . There exists a constant $c > 0$, independent of h , such that,

$$\|A_h^\ell - \text{Id}\|_{L^\infty(\Gamma)} \leq ch^{r+1} \quad \text{and} \quad \left\| 1 - \frac{1}{J_b^\ell} \right\|_{L^\infty(\Gamma)} \leq ch^{r+1}. \quad (3.7)$$

4 Finite element approximation

In this section, is presented the finite element approximation of problem (1.1) using a \mathbb{P}^k -Lagrange finite element method. We refer to, e.g., [21, 11] and [9, §5] for more details on finite element methods. From now on, we denote Ω_h and Γ_h to refer to $\Omega_h^{(r)}$ and $\Gamma_h^{(r)}$, for any geometrical order $r \geq 1$.

Discrete formulation. Let $k \geq 1$ that denotes the finite element degree. Given a curved mesh $\mathcal{T}_h^{(r)}$, the \mathbb{P}^k -Lagrangian finite element space is given by,

$$\mathbb{V}_h := \left\{ \chi \in C^0(\Omega_h); \chi|_T = \hat{\chi} \circ (F_T^{(r)})^{-1}, \hat{\chi} \in \mathbb{P}^k(\hat{T}), \forall T \in \mathcal{T}_h^{(r)} \right\}.$$

The approximation problem is to find $(\Lambda, U) \in \mathbb{R} \times \mathbb{V}_h$ such that,

$$a_h(U, V) = \Lambda m_h(U, V), \quad \forall V \in \mathbb{V}_h, \quad (4.1)$$

where a_h is the following bilinear form, defined on $\mathbb{V}_h \times \mathbb{V}_h$,

$$a_h(U, V) := \int_{\Omega_h} \nabla U \cdot \nabla V dx + \int_{\Gamma_h} \nabla_{\Gamma_h} U \cdot \nabla_{\Gamma_h} V ds_h + \int_{\Gamma_h} UV ds_h,$$

and m_h is the following bilinear form, defined on $\mathbb{V}_h \times \mathbb{V}_h$,

$$m_h(U, V) = \int_{\Omega_h} UV dx.$$

Remark 4.1. *The discrete problem (4.1) admits an increasing finite sequence of positive discrete eigenvalues $\Lambda_j \in \mathbb{R}_+^*$. There exists a basis of \mathbb{V}_h made of discrete eigenfunctions $\{U_j\}_{j=1}^{\dim(\mathbb{V}_h)}$, which are m_h -orthogonal (see [1, Lemma 7.4.1]).*

Lifted discrete formulation. The lifted finite element space is given by,

$$\mathbb{V}_h^\ell := \{v_h^\ell, v_h \in \mathbb{V}_h\}.$$

We define the lifted bilinear form a_h^ℓ , defined on $\mathbb{V}_h^\ell \times \mathbb{V}_h^\ell$, throughout,

$$a_h(U, V) = a_h^\ell(U^\ell, V^\ell), \quad \forall U, V \in \mathbb{V}_h.$$

By applying (3.3), (3.6) and (3.5), then the expression of a_h^ℓ is given by,

$$a_h^\ell(U^\ell, V^\ell) = \int_{\Omega} \mathcal{G}_h^{(r)}(\nabla U^\ell) \cdot \mathcal{G}_h^{(r)}(\nabla V^\ell) \frac{dx}{J_h^\ell} + \int_{\Gamma} A_h^\ell \nabla_{\Gamma} u_h^\ell \cdot \nabla_{\Gamma} v_h^\ell ds + \int_{\Gamma} U^\ell V^\ell \frac{ds}{J_b^\ell}.$$

In a similar way, using (3.2), we define the expression of m_h^ℓ , defined on $\mathbb{V}_h^\ell \times \mathbb{V}_h^\ell$, throughout $m_h(U, V) = m_h^\ell(U^\ell, V^\ell)$ for $U, V \in \mathbb{V}_h$, as follows,

$$m_h^\ell(U^\ell, V^\ell) = \int_{\Omega} UV \frac{dx}{J_h^\ell} = m_h(U, V).$$

Thus, we define the lifted formulation of Problem (4.1) given by: find $(\Lambda, U^\ell) \in \mathbb{R} \times \mathbb{V}_h^\ell$ such that,

$$a_h^\ell(U^\ell, V) = \Lambda m_h^\ell(U^\ell, V), \quad \forall V \in \mathbb{V}_h^\ell. \quad (4.2)$$

Remark 4.2. *The lifted problem (4.2) shares the same eigenvalues as the discrete problem (4.1), denoted $\{\Lambda_j\}_{j=1}^{\dim(\mathbb{V}_h)}$, which are associated to the lift of the eigenfunctions of the discrete formulation (2.1), denoted $\{U_j^\ell\}_{j=1}^{\dim(\mathbb{V}_h)}$. Throughout the rest of this work, we suppose that the discrete eigenfunctions satisfy that $\|U_j^\ell\|_{m_h^\ell} = 1$, for all $j = 1, \dots, \dim(\mathbb{V}_h)$.*

5 Error analysis

First of all, the exact eigenvalues are ordered increasingly with their multiplicities. Let $i \in \mathbb{N}^*$. The aim of this work is to estimate the error produced when approximating the eigenvalue λ_i of multiplicity N and its corresponding eigenfunctions, $\{u_j\}_{j \in J}$ where $J = \{i, \dots, i + N - 1\}$, using a \mathbb{P}^k finite element method on a curved mesh Ω_h with a geometrical order $r \geq 1$. These estimations are given in the following theorem, which is proved in the following sub-sections.

To this end, denote $\{\Lambda_j\}_{j=1}^{\dim(\mathbb{V}_h)}$ the set of all the discrete eigenvalue. Each eigenvalue Λ_j is associated to an eigenspace $\mathbb{E}_{\Lambda_j}^\ell$ in \mathbb{V}_h^ℓ , which is the set of all the discrete eigenfunctions associated to Λ_j . Let $\mathbb{F}_h^\ell := \bigoplus_{j \in J} \mathbb{E}_{\Lambda_j}^\ell$ be the space containing all the eigenspaces associated to $\{\Lambda_j\}_{j \in J}$.

Throughout this section, c refers to a positive constant independent of the mesh size h and c_{λ_i} refers to a positive constant dependent of the eigenvalue λ_i and independent of h . From now on, the domain Ω , is assumed to be at least \mathcal{C}^{k+1} regular such that the exact eigenfunctions of Problem (1.1) are in $H^{k+1}(\Omega, \Gamma)$.

Theorem 5.1. *Let λ_i be an eigenvalue of multiplicity N with its corresponding eigenfunctions, $\{u_p\}_{p \in J}$ where $J = \{i, \dots, i + N - 1\}$, relatively to Problem (2.1). Then, for any $j \in J$, there exists $c_{\lambda_i} > 0$,*

$$|\lambda_j - \Lambda_j| \leq c_{\lambda_i}(h^{2k} + h^{r+1}), \quad (5.1)$$

where Λ_j is a discrete eigenvalue relatively to Problem (4.1). Additionally, there exists $c_{\lambda_i} > 0$ for any $j \in J$ such that,

$$\inf_{U \in \mathbb{F}_h^\ell} \|u_j - U\|_{L^2(\Omega)} \leq c_{\lambda_i}(h^{k+1} + h^{r+1/2}), \quad (5.2)$$

$$\inf_{U \in \mathbb{F}_h^\ell} \|u_j - U\|_{H^1(\Omega, \Gamma)} \leq c_{\lambda_i}(h^k + h^{r+1/2}), \quad (5.3)$$

where \mathbb{F}_h^ℓ is the space containing all the eigenspaces associated to $\{\Lambda_j\}_{j \in J}$.

Remark 5.1. *In a similar manner, there exists $c_{\lambda_i} > 0$ such that,*

$$\inf_{u \in \mathbb{E}_{\lambda_i}} \|U - u\|_{L^2(\Omega)} \leq c_{\lambda_i}(h^{k+1} + h^{r+1/2}), \quad \inf_{u \in \mathbb{E}_{\lambda_i}} \|U - u\|_{H^1(\Omega, \Gamma)} \leq c_{\lambda_i}(h^k + h^{r+1/2}),$$

where $U \in \mathbb{V}_h^\ell$ is a discrete eigenfunction associated to Λ_j and \mathbb{E}_{λ_i} is the eigenspace of λ_i . These estimations, which are analogous to those presented in Theorem 5.1, are a consequence of Lemma 5.4 in Section 5.4.

In order to prove this theorem, we will proceed in several steps. In a nutshell, the main steps of the proof are to first estimate the so-called geometric error, second calculate a preliminary eigenvalue estimation, third estimate the eigenfunction error, and finally combine the last two steps to improve the eigenvalue error.

5.1 Geometric error

Before estimating the geometric error, we need to present the following corollary, which plays a key role in the remaining of the article (see [9, Lemma 2]).

Corollary 5.1. *Let $v \in H^1(\Omega)$ and $w \in H^2(\Omega)$, then, for a sufficiently small h , there exists $c > 0$ such that the following inequalities hold,*

$$\|v\|_{L^2(B_h^\ell)} \leq ch^{1/2}\|v\|_{H^1(\Omega)}, \quad (5.4)$$

$$\|\nabla w\|_{L^2(B_h^\ell)} \leq ch^{1/2}\|w\|_{H^2(\Omega)}, \quad (5.5)$$

where $B_h^\ell = \left\{ T^{(e)} \in \mathcal{T}_h^{(e)}; T^{(e)} \text{ has at least 2 vertices on } \Gamma \right\}$.

We present the following property on the domain B_h^ℓ , which plays a key role in the geometric error estimation,

$$\frac{1}{J_h^\ell} - 1 = 0 \quad \text{and} \quad \mathcal{G}_h^{(r)} - Id = 0, \quad \text{in } \Omega \setminus B_h^\ell. \quad (5.6)$$

To estimate the geometric error produced while approximating a domain by a mesh of order $r \geq 1$, we bound the difference between the two bilinear forms a and a_h^ℓ (resp. m and m_h^ℓ).

Proposition 5.1. *Let $v, w \in \mathbb{V}_h^\ell$. Then there exists $c > 0$ such that,*

$$|(a - a_h^\ell)(v, w)| \leq c(h^r \|\nabla v\|_{L^2(B_h^\ell)} \|\nabla w\|_{L^2(B_h^\ell)} + h^{r+1} \|v\|_{H^1(\Gamma)} \|w\|_{H^1(\Gamma)}), \quad (5.7)$$

$$|(m - m_h^\ell)(v, w)| \leq ch^{r+1} \|v\|_{H^1(\Omega)} \|w\|_{H^1(\Omega)}. \quad (5.8)$$

Proof. The proof of (5.7) is detailed in [9, Proposition 6.3], given using (3.4) and (3.7). To prove (5.8), consider $v, w \in \mathbb{V}_h^\ell$. Using (5.6) and (3.4), we have,

$$\begin{aligned} |(m - m_h^\ell)(v, w)| &= \left| \int_{\Omega} vw \left(1 - \frac{1}{J_h^\ell}\right) dx \right| = \left| \int_{B_h^\ell} vw \left(1 - \frac{1}{J_h^\ell}\right) dx \right| \\ &\leq \left\| 1 - \frac{1}{J_h^\ell} \right\|_{L^\infty(B_h^\ell)} \|v\|_{L^2(B_h^\ell)} \|w\|_{L^2(B_h^\ell)} \leq ch^r \|v\|_{L^2(B_h^\ell)} \|w\|_{L^2(B_h^\ell)}. \end{aligned}$$

Since $v, w \in \mathbb{V}_h^\ell \subset H^1(\Omega, \Gamma)$, we apply (5.4) as follows,

$$|(m - m_h^\ell)(v, w)| \leq ch^r \left(h^{1/2} \|v\|_{H^1(\Omega)} \right) \left(h^{1/2} \|w\|_{H^1(\Omega)} \right) \leq ch^{r+1} \|v\|_{H^1(\Omega)} \|w\|_{H^1(\Omega)}. \quad \square$$

Corollary 5.2. *Considering a sufficiently small mesh size $h > 0$, the boundary of the mesh domain Γ_h is inside the tubular neighbourhood $\mathcal{U}_{\delta\Gamma}$, defined in Proposition 2.1. Then, there exists $c > 0$ such that,*

$$\begin{aligned} \|\cdot\|_{a_h^\ell} &\leq (1 + ch^r) \|\cdot\|_a, & \|\cdot\|_a &\leq (1 + ch^r) \|\cdot\|_{a_h^\ell}, \\ \|\cdot\|_{m_h^\ell} &\leq (1 + ch^r) \|\cdot\|_m, & \|\cdot\|_m &\leq (1 + ch^r) \|\cdot\|_{m_h^\ell}, \end{aligned}$$

where the norms $\|u\|_a, \|u\|_m, \|u\|_{a_h^\ell}, \|u\|_{m_h^\ell}$ are associated to the bilinear forms a, a_h^ℓ, m and m_h^ℓ , respectively. Consequently, the norms $\|\cdot\|_{a_h^\ell}$ and $\|\cdot\|_a$ (resp. $\|\cdot\|_{m_h^\ell}$ and $\|\cdot\|_m$) are equivalent.

Proof. This proof is an adaptation of the proof of [6, Corollary 2.3], which is detailed for readers convenience. Let $u \in H^1(\Omega, \Gamma)$, one has,

$$\|u\|_{a_h^\ell}^2 - \|u\|_a^2 = a_h^\ell(u, u) - a(u, u) = (a_h^\ell - a)(u, u).$$

Then, we deduce that,

$$\|u\|_{a_h^\ell}^2 \leq \|u\|_a^2 + |(a_h^\ell - a)(u, u)| \leq (1 + ch^r) \|u\|_a^2,$$

where we used the geometric error estimation (5.7). Taking its square root, it follows that,

$$\|u\|_{a_h^\ell} \leq \sqrt{(1 + ch^r)} \|u\|_a \leq (1 + ch^r) \|u\|_a,$$

since for any $x \geq 0$, $1 + x \leq (1 + \frac{1}{2}x)^2$. In a similar manner, the rest of the inequalities can be proved, by using (5.7) and (5.8). \square

5.2 Preliminary eigenvalue estimate

A preliminary eigenvalue error estimation is needed before proceeding with the error estimation. It has to be noted that a similar result was established in [6, Th. 3.3], in a different context. For sake of completeness, we detail the proof of the following proposition.

Proposition 5.2. *Let λ_i be an exact eigenvalue of multiplicity N of Problem (2.1), such that $\lambda_j = \lambda_i$, for any $j \in \mathbf{J} = \{i, \dots, i + N - 1\}$. Let $\{\Lambda_p\}_{p=1}^{\dim(\mathbb{V}_h)}$ be the set of discrete eigenvalues relatively to Problem (4.1). Then, for any $j \in \mathbf{J}$, there exists $c_{\lambda_i} > 0$ such that,*

$$|\lambda_j - \Lambda_j| \leq c_{\lambda_i}(h^{2k} + h^r). \quad (5.9)$$

Proof. Let $j \in \mathbf{J}$. To estimate the error $|\lambda_j - \Lambda_j|$, we introduce the following intermediate formulation: Find $(\tilde{\lambda}, \tilde{U}) \in \mathbb{R}^+ \times \mathbb{V}_h^\ell$, such that,

$$a(\tilde{U}, v) = \tilde{\lambda}m(\tilde{U}, v) \quad \forall v \in \mathbb{V}_h^\ell. \quad (5.10)$$

Problem (5.10) has a finite number of solutions. Denote $\tilde{\Lambda}_p \in \mathbb{R}$ its eigenvalues, for $p = 1, \dots, \dim(\mathbb{V}_h^\ell)$. Then for $j \in \mathbf{J}$, we separate the eigenvalue error as follows,

$$|\lambda_j - \Lambda_j| \leq |\lambda_j - \tilde{\Lambda}_j| + |\tilde{\Lambda}_j - \Lambda_j|,$$

and estimate each term separately.

For the estimation of $|\lambda_j - \tilde{\Lambda}_j|$, note that the eigenvalue problem (5.10) is in a conformal, coercive and consistent setting. Indeed, the variational form is defined using the same bilinear forms a and m as in the initial formulation (2.1), with the approximation space $\mathbb{V}_h^\ell \subset \mathbf{H}^1(\Omega, \Gamma)$. Thus, we refer to the detailed explanation in [21, chapter 3.3] to obtain the following classical estimation,

$$|\lambda_j - \tilde{\Lambda}_j| \leq c_{\lambda_i} h^{2k}. \quad (5.11)$$

From the inequality 5.11, we notice that for any $j \in \mathbf{J}$, $0 < \tilde{\Lambda}_j \leq c_{\lambda_i}$.

To estimate $|\tilde{\Lambda}_j - \Lambda_j|$, we proceed in an analogous way as in [6, Lemma 3.1]. Note that, by [21, Proposition 3.63], the discrete eigenvalues can be written as follows,

$$\Lambda_j = \min_{E \in V_j} \max_{v \in E} R_{a_h^\ell}(v) \quad \text{and} \quad \tilde{\Lambda}_j = \min_{E \in V_j} \max_{v \in E} R_a(v), \quad (5.12)$$

where the associated Rayleigh quotients are written as follows,

$$R_{a_h^\ell}(v) = \frac{a_h^\ell(v, v)}{m_h^\ell(v, v)} \quad \text{and} \quad R_a(v) = \frac{a(v, v)}{m(v, v)},$$

where V_j is the set of all sub-spaces of \mathbb{V}_h^ℓ of dimension j .

Consider $E \in V_j$. By definition of the Rayleigh quotient and using the norm equivalence in Corollary 5.2, we can deduce for any $v \in E$,

$$R_{a_h^\ell}(v) = \frac{a_h^\ell(v, v)}{m_h^\ell(v, v)} \leq \frac{(1 + ch^r)^2 a(v, v)}{\frac{m(v, v)}{(1 + ch^r)^2}} = (1 + ch^r)^4 R_a(v).$$

Using (5.12), it follows that,

$$\Lambda_j \leq \min_{E \in V_j} \max_{v \in E} (1 + ch^r)^4 R_a(v) = (1 + ch^r)^4 \tilde{\Lambda}_j.$$

Then, $\Lambda_j \leq \tilde{\Lambda}_j + ch^r \tilde{\Lambda}_j$, and we have, $\Lambda_j - \tilde{\Lambda}_j \leq ch^r \tilde{\Lambda}_j \leq c_{\lambda_i} h^r$. In a similar manner, we can prove that $\tilde{\Lambda}_j - \Lambda_j \leq c_{\lambda_i} h^r$. To conclude, we combine these two inequalities as follows,

$$|\Lambda_j - \tilde{\Lambda}_j| \leq c_{\lambda_i} h^r. \quad (5.13)$$

To conclude, we combine (5.13) and (5.11) to arrive at (5.9). \square

Remark 5.2. *As a result of the estimation 5.9, the eigenvalues $\{\lambda_j\}_{j \in J}$ are only approximated by the set of discrete eigenvalues $\{\Lambda_j\}_{j \in J}$. Consequently, for a sufficiently small mesh step h , the following quantity, which appears in the eigenfunction estimations, is finite,*

$$\mu_J = \max_{j \in J} \max_{p \notin J} \left| \frac{\lambda_j}{\Lambda_p - \lambda_j} \right| < \infty.$$

Additionally, the set of eigenvalues $\{\Lambda_j\}_{j \in J}$ is separated from the rest of the continuous spectrum, i.e.,

$$\lambda_{i-1} < \Lambda_i \quad \text{and} \quad \Lambda_{i+N-1} < \lambda_{i+N}.$$

Furthermore, this set of discrete eigenvalues $\{\Lambda_j\}_{j \in J}$ can be bounded independently from the mesh size h . Indeed, there exists $c_{\lambda_i} > 0$, such that, $|\Lambda_j| \leq c_{\lambda_i}$, for all $j \in J$. We refer to [8, page 6], [22, §2.3], [23, page 3], [28, Section 3.2] and [6, remark 3.4].

5.3 Eigenfunction error estimations

In this section, is presented the proof of the estimations (5.2) and (5.3) of Theorem 5.1. To begin with, we recall that $\mathbb{F}_h^\ell = \oplus_{j \in J} \mathbb{E}_{\Lambda_j}^\ell = \oplus_{j \in J} \text{span} \{U_j^\ell\}$. We define the following projections, which are a useful tool in the eigenfunction error estimates (see [21, §1.6.3]).

Definition 5.1. *We define the following projections:*

- Let $\Pi_h : \mathbf{H}^1(\Omega, \Gamma) \rightarrow \mathbb{V}_h^\ell$ be the Riesz projection, such that $\forall v \in \mathbf{H}^1(\Omega, \Gamma)$, there exists a unique finite element function $\Pi_h(v) \in \mathbb{V}_h^\ell$ that satisfies,

$$a_h^\ell(\Pi_h(v), w) = a_h^\ell(v, w), \quad \forall w \in \mathbb{V}_h^\ell.$$

- Let $\mathcal{P}_{a_h^\ell} : \mathbf{H}^1(\Omega, \Gamma) \rightarrow \mathbb{F}_h^\ell$ be the orthogonal projection with respect to a_h^ℓ onto \mathbb{F}_h^ℓ , such that for all $v \in \mathbf{H}^1(\Omega, \Gamma)$,

$$a_h^\ell(\mathcal{P}_{a_h^\ell}(v), w) = a_h^\ell(v, w), \quad \forall w \in \mathbb{F}_h^\ell.$$

- Let $\mathcal{P}_{m_h^\ell} : \mathbf{H}^1(\Omega, \Gamma) \rightarrow \mathbb{F}_h^\ell$ be the orthogonal projection with respect to m_h^ℓ onto \mathbb{F}_h^ℓ , such that for all $v \in \mathbf{H}^1(\Omega, \Gamma)$,

$$m_h^\ell(\mathcal{P}_{m_h^\ell}(v), w) = m_h^\ell(v, w), \quad \forall w \in \mathbb{F}_h^\ell.$$

Remark 5.3. *Note that the previous orthogonal projections satisfy the following relation (see [6, Section 2.4] and [22, Lemma 2.2]),*

$$\mathcal{P}_{a_h^\ell} = \mathcal{P}_{m_h^\ell} \circ \Pi_h.$$

The key idea, in proof of the estimations (5.2) and (5.2), is to separate the error in two terms for both norms as follows,

$$\inf_{U \in \mathbb{F}_h^\ell} \|u_j - U\| \leq \|u_j - \Pi_h u_j\| + \|\Pi_h u_j - \mathcal{P}_{a_h^\ell} u_j\|.$$

The first term will be bounded using a classical interpolation result (see [21, §1.6.3]). If $u_j \in \mathbb{H}^{k+1}(\Omega, \Gamma)$, by definition of the Riesz projection Π_h , there exists $c > 0$ such that,

$$\|u_j - \Pi_h u_j\|_{a_h^\ell} = \inf_{v \in \mathbb{V}_h^\ell} \|u_j - v\|_{a_h^\ell} \leq ch^k \|u_j\|_{\mathbb{H}^{k+1}(\Omega, \Gamma)}. \quad (5.14)$$

Using an Aubin-Nitsche argument as proved in Appendix C, there exists $c > 0$ such that,

$$\|u_j - \Pi_h u_j\|_{m_h^\ell} \leq ch^{k+1}. \quad (5.15)$$

As for the second term, we recall that $\{U_p^\ell\}_{p=1}^{\dim(\mathbb{V}_h)}$ forms an orthonormal basis of \mathbb{V}_h^ℓ with respect to m_h^ℓ . The lifted space finite element space can be decomposed as follows $\mathbb{V}_h^\ell := \mathbb{F}_h^\ell \oplus \mathbb{S}_h^\ell$, where $\mathbb{F}_h^\ell := \oplus_{j \in \mathbb{J}} \text{span} U_j^\ell$ and $\mathbb{S}_h^\ell := \oplus_{p \notin \mathbb{J}} \text{span} U_p^\ell$ are orthogonal spaces with respect to m_h^ℓ . We denote,

$$W := \Pi_h u_j - \mathcal{P}_{a_h^\ell} u_j = \Pi_h u_j - \mathcal{P}_{m_h^\ell} \circ \Pi_h u_j. \quad (5.16)$$

Since $\mathcal{P}_{m_h^\ell}$ is the orthogonal projection over \mathbb{F}_h^ℓ with respect to m_h^ℓ , then we have,

$$W \in \mathbb{S}_h^\ell, \quad m_h^\ell(W, U_j^\ell) = 0, \quad \forall j \in \mathbb{J}.$$

Consequently, $W = \sum_{p \notin \mathbb{J}} \beta_p U_p^\ell$, where we denote the coefficients $\beta_p := m_h^\ell(W, U_p^\ell)$, for all $p \notin \mathbb{J}$. Then the m_h^ℓ norm of W is given as follows,

$$\|W\|_{m_h^\ell}^2 = \sum_{p \notin \mathbb{J}} \beta_p^2, \quad (5.17)$$

since $\{U_p^\ell\}_{p \notin \mathbb{J}}$ forms an orthonormal basis of \mathbb{S}_h^ℓ for the product m_h^ℓ .

In the following propositions the a_h^ℓ and m_h^ℓ norms of W will be evaluated in order to bound the error afterwards. We introduce the following notation,

$$Z := \sum_{p \notin \mathbb{J}} \frac{\lambda_i}{\Lambda_p - \lambda_i} \beta_p U_p^\ell, \quad (5.18)$$

where Λ_p is a discrete eigenvalue with its associated eigenfunction U_p^ℓ , and λ_i is the exact eigenvalue.

Proposition 5.3. *Let $j \in \mathbb{J}$ and u_j be an exact eigenfunction associated with λ_i . The norms of W , given in (5.16), can be expressed as follows,*

$$\|W\|_{m_h^\ell}^2 = m_h^\ell(u_j - \Pi_h u_j, Z) + (m - m_h^\ell)(u_j, Z) + \frac{1}{\lambda_i} (a_h^\ell - a)(u_j, Z), \quad (5.19)$$

$$\|W\|_{a_h^\ell}^2 = \lambda_i m_h^\ell(u_j - \Pi_h u_j, W) + \lambda_i \|W\|_{m_h^\ell}^2 + \lambda_i (m - m_h^\ell)(u_j, W) + (a_h^\ell - a)(u_j, W). \quad (5.20)$$

Proof. This proof is inspired from [6, Lemma 4.1], but for sake of completeness we detail it. The main difference is that in our case, we do not consider a surface problem as in [6] and the eigenfunctions $\{u_j\}_{j \in \mathbb{J}}$ are on Ω .

By Equation (5.17), the m_h^ℓ norm of W is written as follows,

$$\|W\|_{m_h^\ell}^2 = \sum_{p \notin \mathbb{J}} \beta_p^2 = \sum_{p \notin \mathbb{J}} \beta_p m_h^\ell(W, U_p^\ell). \quad (5.21)$$

To prove (5.19), we try to estimate $m_h^\ell(W, U_p^\ell)$, for $p \notin J$. By Remark 5.3, $\mathcal{P}_{a_h^\ell} = \mathcal{P}_{m_h^\ell} \circ \Pi_h$, and we get for $p \notin J$,

$$m_h^\ell(\mathcal{P}_{a_h^\ell} v, U_p^\ell) = m_h^\ell(\mathcal{P}_{m_h^\ell}(\Pi_h v), U_p^\ell) = 0, \quad \forall v \in H^1(\Omega, \Gamma). \quad (5.22)$$

Using (5.22), we get for $p \notin J$,

$$m_h^\ell(W, U_p^\ell) = m_h^\ell(\Pi_h u_j - \mathcal{P}_{a_h^\ell} u_j, U_p^\ell) = m_h^\ell(\Pi_h(u_j), U_p^\ell).$$

The next step is to estimate $m_h^\ell(\Pi_h u_j, U_p^\ell)$. We denote Λ_p a discrete eigenvalue associated to $U_p^\ell \in \mathbb{S}_h^\ell$ such that,

$$\Lambda_p m_h^\ell(V, U_p^\ell) = a_h^\ell(V, U_p^\ell), \quad \forall V \in \mathbb{V}_h^\ell.$$

Taking in the latter equation $V = \Pi_h u_j \in \mathbb{V}_h^\ell$, we get by using the definition of Π_h ,

$$\Lambda_p m_h^\ell(\Pi_h u_j, U_p^\ell) = a_h^\ell(\Pi_h u_j, U_p^\ell) = a_h^\ell(u_j, U_p^\ell) = a(u_j, U_p^\ell) + (a_h^\ell - a)(u_j, U_p^\ell).$$

Since u_j is an exact eigenfunction associated to λ_i of Problem (2.1), we get,

$$\begin{aligned} \Lambda_p m_h^\ell(\Pi_h u_j, U_p^\ell) &= \lambda_i m(u_j, U_p^\ell) + (a_h^\ell - a)(u_j, U_p^\ell) \\ &= \lambda_i m_h^\ell(u_j, U_p^\ell) + \lambda_i(m - m_h^\ell)(u_j, U_p^\ell) + (a_h^\ell - a)(u_j, U_p^\ell), \end{aligned}$$

where we added and subtracted $\lambda_i m_h^\ell(u_j, U_p^\ell)$.

Subtracting $\lambda_i m_h^\ell(\Pi_h u_j, U_p^\ell)$ on both sides of the equation, we get,

$$(\Lambda_p - \lambda_i) m_h^\ell(\Pi_h u_j, U_p^\ell) = \lambda_i m_h^\ell(u_j - \Pi_h u_j, U_p^\ell) + \lambda_i(m - m_h^\ell)(u_j, U_p^\ell) + (a_h^\ell - a)(u_j, U_p^\ell).$$

For any $p \notin J$, $\Lambda_p - \lambda_i \neq 0$, then we have,

$$\begin{aligned} m_h^\ell(\Pi_h u_j, U_p^\ell) &= \frac{1}{\Lambda_p - \lambda_i} \{ \lambda_i m_h^\ell(u_j - \Pi_h u_j, U_p^\ell) + \lambda_i(m - m_h^\ell)(u_j, U_p^\ell) + (a_h^\ell - a)(u_j, U_p^\ell) \} \\ &= m_h^\ell(u_j - \Pi_h u_j, \frac{\lambda_i}{\Lambda_p - \lambda_i} U_p^\ell) + (m - m_h^\ell)(u_j, \frac{\lambda_i}{\Lambda_p - \lambda_i} U_p^\ell) + \frac{1}{\lambda_i} (a_h^\ell - a)(u_j, \frac{\lambda_i}{\Lambda_p - \lambda_i} U_p^\ell). \end{aligned}$$

To arrive to (5.19), we replace the latter expression in (5.21) as follows,

$$\begin{aligned} \|W\|_{m_h^\ell}^2 &= \sum_{p \in \{1, \dots, \dim(\mathbb{V}_h)\} \setminus J} \beta_p \left(m_h^\ell(u_j - \Pi_h u_j, \frac{\lambda_i}{\Lambda_p - \lambda_i} U_p^\ell) \right. \\ &\quad \left. + (m - m_h^\ell)(u_j, \frac{\lambda_i}{\Lambda_p - \lambda_i} U_p^\ell) + \frac{1}{\lambda_i} (a_h^\ell - a)(u_j, \frac{\lambda_i}{\Lambda_p - \lambda_i} U_p^\ell) \right). \end{aligned}$$

The proof of (5.20) is a tad similar to the latter one. Keeping in mind that $W = (\text{Id} - \mathcal{P}_{m_h^\ell}) \Pi_h u_j$, its a_h^ℓ -norm is written as follows,

$$\begin{aligned} \|W\|_{a_h^\ell}^2 &= a_h^\ell(W, W) = a_h^\ell((\text{Id} - \mathcal{P}_{m_h^\ell}) \Pi_h u_j, (\text{Id} - \mathcal{P}_{m_h^\ell}) \Pi_h u_j) \\ &= a_h^\ell(\Pi_h u_j, (\text{Id} - \mathcal{P}_{m_h^\ell}) \Pi_h u_j) - a_h^\ell(\mathcal{P}_{m_h^\ell} \Pi_h u_j, (\text{Id} - \mathcal{P}_{m_h^\ell}) \Pi_h u_j). \end{aligned}$$

Note that, for any $V \in \mathbb{F}_h^\ell$, we have,

$$a_h^\ell((\text{Id} - \mathcal{P}_{m_h^\ell}) \Pi_h u_j, V) = a_h^\ell(\Pi_h u_j, V) - a_h^\ell(\mathcal{P}_{m_h^\ell} \circ \Pi_h u_j, V) = a_h^\ell(u_j, V) - a_h^\ell(\mathcal{P}_{a_h^\ell} u_j, V) = 0,$$

where we used the definitions of the orthogonal projections Π_h and $\mathcal{P}_{a_h^\ell}$. Thus, taking $V = \mathcal{P}_{m_h^\ell} \Pi_h u_j \in \mathbb{F}_h^\ell$, $a_h^\ell(\mathcal{P}_{m_h^\ell} \Pi_h u_j, (\text{Id} - \mathcal{P}_{m_h^\ell}) \Pi_h u_j) = 0$. Then, the latter equation becomes,

$$\|W\|_{a_h^\ell}^2 = a_h^\ell(\Pi_h u_j, (\text{Id} - \mathcal{P}_{m_h^\ell}) \Pi_h u_j) = a_h^\ell(u_j, (\text{Id} - \mathcal{P}_{m_h^\ell}) \Pi_h u_j) = a_h^\ell(u_j, W),$$

where we used the definition of the orthogonal projection Π_h with respect to a_h^ℓ , given in Definition 5.1. Adding and subtracting $a(u_j, W)$, we get,

$$\|W\|_{a_h^\ell}^2 = a_h^\ell(u_j, W) = a(u_j, W) + (a_h^\ell(u_j, W) - a(u_j, W)) = \lambda_i m(u_j, W) + (a_h^\ell - a)(u_j, W).$$

Since u_j is an exact eigenfunction associated to λ_i , the latter equation holds. Adding and subtracting $\lambda_i m_h^\ell(u_j, W)$, we have,

$$\|W\|_{a_h^\ell}^2 = \lambda_i m_h^\ell(u_j, W) + \lambda_i (m - m_h^\ell)(u_j, W) + (a_h^\ell - a)(u_j, W). \quad (5.23)$$

Notice that $W = \sum_{p \notin J} \beta_p U_p^\ell$, then by applying (5.22), we have $m_h^\ell(\mathcal{P}_{a_h^\ell} u_j, W) = 0$. Then, we notice that,

$$\begin{aligned} \lambda_i m_h^\ell(u_j, W) &= \lambda_i m_h^\ell(u_j, W) - \lambda_i m_h^\ell(\mathcal{P}_{a_h^\ell} u_j, W) \\ &= \lambda_i m_h^\ell(u_j - \Pi_h u_j, W) + \lambda_i m_h^\ell(\Pi_h u_j - \mathcal{P}_{a_h^\ell} u_j, W) = \lambda_i m_h^\ell(u_j - \Pi_h u_j, W) + \lambda_i m_h^\ell(W, W), \end{aligned}$$

where we added and subtracted $\lambda_i m_h^\ell(\Pi_h u_j, W)$. Thus after replacing the latter equation in (5.23), we get exactly (5.20),

$$\|W\|_{a_h^\ell}^2 = \lambda_i m_h^\ell(u_j - \Pi_h u_j, W) + \lambda_i \|W\|_{m_h^\ell}^2 + \lambda_i (m - m_h^\ell)(u_j, W) + (a_h^\ell - a)(u_j, W).$$

□

The following proposition is one of the main novelties of this work. The general idea of bounding the norms of W can be seen in [6, 22, 8] for different problems.

Proposition 5.4. *Under the assumptions of Proposition 5.3, there exists $c_{\lambda_i} > 0$ such that,*

$$\|W\|_{m_h^\ell} \leq c_{\lambda_i} \|u_j - \Pi_h u_j\|_{m_h^\ell} + c_{\lambda_i} h^{r+1/2} \|u_j\|_{\mathbb{H}^2(\Omega, \Gamma)}, \quad (5.24)$$

$$\|W\|_{a_h^\ell} \leq c_{\lambda_i} \|u_j - \Pi_h u_j\|_{m_h^\ell} + c_{\lambda_i} h^{r+1/2} \|u_j\|_{\mathbb{H}^2(\Omega, \Gamma)}, \quad (5.25)$$

where the expression of W is given in (5.16).

Proof. This proof is decomposed into three steps.

1. Using the geometric error estimates (5.7) and (5.8), the m_h^ℓ -norm of W , given by (5.19), can be estimated as follows,

$$\begin{aligned} \|W\|_{m_h^\ell}^2 &= m_h^\ell(u_j - \Pi_h u_j, Z) + \left[(m - m_h^\ell) + \frac{1}{\lambda_i} (a_h^\ell - a) \right] (u_j, Z) \\ &\leq c \|u_j - \Pi_h u_j\|_{m_h^\ell} \|Z\|_{m_h^\ell} + c h^{r+1} \|u_j\|_{\mathbb{H}^1(\Omega)} \|Z\|_{\mathbb{H}^1(\Omega)} \\ &\quad + \frac{c}{\lambda_i} \left(h^r \|\nabla u_j\|_{\mathbb{L}^2(B_h^\ell)} \|\nabla Z\|_{\mathbb{L}^2(B_h^\ell)} + h^{r+1} \|u_j\|_{\mathbb{H}^1(\Gamma)} \|Z\|_{\mathbb{H}^1(\Gamma)} \right), \end{aligned}$$

where the expression of Z is given in (5.18). Keeping in mind that the discrete eigenfunctions are m_h^ℓ -orthogonal, by Remark (5.2) of μ_J , we have,

$$\|Z\|_{m_h^\ell}^2 = \sum_{p \notin J} \left(\frac{\lambda_i}{\Lambda_p - \lambda_i} \right)^2 \beta_p^2 \|U_p^\ell\|_{m_h^\ell}^2 \leq \mu_J^2 \|W\|_{m_h^\ell}^2. \quad (5.26)$$

Since U_p^ℓ is a discrete eigenfunction associated to Λ_p , then for any $q \neq p$, we have $a_h^\ell(U_p^\ell, U_q^\ell) = \Lambda_p m_h^\ell(U_p^\ell, U_q^\ell)$. This implies that, that the discrete eigenfunctions $\{U_p^\ell\}_{p \notin J}$ are a_h^ℓ -orthogonal, and that the following inequality holds,

$$\|Z\|_{a_h^\ell}^2 \leq \mu_J^2 \|W\|_{a_h^\ell}^2.$$

As a consequence, one can deduce the following,

$$\|\nabla Z\|_{L^2(B_h^\ell)} \leq \mu_J \|W\|_{a_h^\ell} \quad \text{and} \quad \|Z\|_{H^1(\Gamma)} \leq \mu_J \|W\|_{a_h^\ell}. \quad (5.27)$$

Additionally, we get,

$$\|Z\|_{H^1(\Omega)} \leq \|Z\|_{a_h^\ell} + \|Z\|_{m_h^\ell} \leq \mu_J \|W\|_{a_h^\ell} + \mu_J \|W\|_{m_h^\ell}.$$

Using the latter inequality alongside (5.26) and (5.27), we get,

$$\begin{aligned} \|W\|_{m_h^\ell}^2 &\leq c\mu_J \|u_j - \Pi_h u_j\|_{m_h^\ell} \|W\|_{m_h^\ell} + ch^{r+1} \mu_J \|u_j\|_{H^1(\Omega)} (\|W\|_{a_h^\ell} + \|W\|_{m_h^\ell}) \\ &\quad + \frac{c}{\lambda_i} \left(h^r \|\nabla u_j\|_{L^2(B_h^\ell)} + h^{r+1} \|u_j\|_{H^1(\Gamma)} \right) \mu_J \|W\|_{a_h^\ell}. \end{aligned}$$

Since the exact eigenfunctions u_j belongs to $H^2(\Omega, \Gamma)$, by applying (5.5), we obtain,

$$\begin{aligned} \|W\|_{m_h^\ell}^2 &\leq c\mu_J \|u_j - \Pi_h u_j\|_{m_h^\ell} \|W\|_{m_h^\ell} + ch^{r+1} \mu_J \|u_j\|_{H^1(\Omega)} \|W\|_{m_h^\ell} \\ &\quad + c \left(1 + \frac{1}{\lambda_i} \right) \mu_J h^{r+1} \|u_j\|_{H^1(\Omega, \Gamma)} \|W\|_{a_h^\ell} + c\mu_J \frac{1}{\lambda_i} h^{r+1/2} \|u_j\|_{H^2(\Omega, \Gamma)} \|W\|_{a_h^\ell} \\ &\leq c\mu_J \|u_j - \Pi_h u_j\|_{m_h^\ell} \|W\|_{m_h^\ell} + ch^{r+1} \mu_J \|u_j\|_{H^1(\Omega)} \|W\|_{m_h^\ell} \\ &\quad + c\mu_J h^{r+1} \|u_j\|_{H^1(\Omega, \Gamma)} \|W\|_{a_h^\ell} + c\mu_J \frac{1}{\lambda_i} h^{r+1/2} \|u_j\|_{H^2(\Omega, \Gamma)} \|W\|_{a_h^\ell}. \end{aligned}$$

Young's inequality, which states that, for all $\epsilon > 0$, $ab \leq \frac{a^2}{\epsilon} + \epsilon b^2$, is applied in the following inequality multiple times as follows, for $\epsilon_1, \epsilon_2 > 0$,

$$\begin{aligned} \|W\|_{m_h^\ell}^2 &\leq 4c\mu_J^2 \|u_j - \Pi_h u_j\|_{m_h^\ell}^2 + \frac{1}{4} \|W\|_{m_h^\ell}^2 + 4ch^{2r+2} \mu_J^2 \|u_j\|_{H^1(\Omega)}^2 + \frac{1}{4} \|W\|_{m_h^\ell}^2 \\ &\quad + \frac{c}{\epsilon_1^2} \mu_J^2 h^{2r+2} \|u_j\|_{H^1(\Omega, \Gamma)}^2 + \epsilon_1^2 \|W\|_{a_h^\ell}^2 + \frac{c}{\epsilon_2^2} \mu_J^2 h^{2r+1} \|u_j\|_{H^2(\Omega, \Gamma)}^2 + \epsilon_2^2 \frac{1}{\lambda_i^2} \|W\|_{a_h^\ell}^2 \\ &\leq c\mu_J^2 \|u_j - \Pi_h u_j\|_{m_h^\ell}^2 + \frac{1}{2} \|W\|_{m_h^\ell}^2 + c \left(\frac{1}{\epsilon_1^2} + \frac{1}{\epsilon_2^2} \right) h^{2r+1} \mu_J^2 \|u_j\|_{H^2(\Omega, \Gamma)}^2 \\ &\quad + \left(\epsilon_1^2 + \frac{\epsilon_2^2}{\lambda_i^2} \right) \|W\|_{a_h^\ell}^2. \end{aligned}$$

Thus, we arrive at,

$$\|W\|_{m_h^\ell}^2 \leq c\mu_J^2 \|u_j - \Pi_h u_j\|_{m_h^\ell}^2 + c\mu_J^2 h^{2r+1} \|u_j\|_{H^2(\Omega, \Gamma)}^2 + \left(\epsilon_1^2 + \frac{\epsilon_2^2}{\lambda_i^2} \right) \|W\|_{a_h^\ell}^2. \quad (5.28)$$

It remains to bound $\|W\|_{a_h^\ell}^2$.

2. To estimate the a_h^ℓ -norm of W , we first recall (5.20) and we use the geometric error estimates (5.7) and (5.8) as follows,

$$\begin{aligned} \|W\|_{a_h^\ell}^2 &\leq c\lambda_i \|u_j - \Pi_h u_j\|_{m_h^\ell} \|W\|_{m_h^\ell} + \lambda_i \|W\|_{m_h^\ell}^2 + c\lambda_i h^{r+1} \|u_j\|_{\mathbb{H}^1(\Omega)} \|W\|_{\mathbb{H}^1(\Omega)} \\ &\quad + ch^r \|\nabla u_j\|_{L^2(B_h^\ell)} \|\nabla W\|_{L^2(B_h^\ell)} + ch^{r+1} \|u_j\|_{\mathbb{H}^1(\Gamma)} \|W\|_{\mathbb{H}^1(\Gamma)}. \end{aligned}$$

Since u_j belongs to $\mathbb{H}^2(\Omega, \Gamma)$, the inequality (5.5) is applied as follows,

$$\begin{aligned} \|W\|_{a_h^\ell}^2 &\leq c\lambda_i \|u_j - \Pi_h u_j\|_{m_h^\ell} \|W\|_{m_h^\ell} + \lambda_i \|W\|_{m_h^\ell}^2 + c\lambda_i h^{r+1} \|u_j\|_{\mathbb{H}^1(\Omega)} (\|W\|_{m_h^\ell} + \|W\|_{a_h^\ell}) \\ &\quad + ch^{r+1/2} \|u_j\|_{\mathbb{H}^2(\Omega, \Gamma)} \|W\|_{a_h^\ell} + ch^{r+1} \|u_j\|_{\mathbb{H}^1(\Gamma)} \|W\|_{a_h^\ell} \\ &\leq c\lambda_i \|u_j - \Pi_h u_j\|_{m_h^\ell} \|W\|_{m_h^\ell} + \lambda_i \|W\|_{m_h^\ell}^2 + c\lambda_i h^{r+1} \|u_j\|_{\mathbb{H}^1(\Omega)} \|W\|_{m_h^\ell} \\ &\quad + c(1 + \lambda_i) h^{r+1/2} \|u_j\|_{\mathbb{H}^2(\Omega, \Gamma)} \|W\|_{a_h^\ell}. \end{aligned}$$

Young's inequality is applied as follows,

$$\begin{aligned} \|W\|_{a_h^\ell}^2 &\leq 4c\lambda_i \|u_j - \Pi_h u_j\|_{m_h^\ell}^2 + \frac{1}{4}\lambda_i \|W\|_{m_h^\ell}^2 + \lambda_i \|W\|_{m_h^\ell}^2 + 4c\lambda_i^2 h^{2r+2} \|u_j\|_{\mathbb{H}^1(\Omega)}^2 \\ &\quad + \frac{1}{4} \|W\|_{m_h^\ell}^2 + 4c(1 + \lambda_i)^2 h^{2r+1} \|u_j\|_{\mathbb{H}^2(\Omega)}^2 + \frac{1}{4} \|W\|_{a_h^\ell}^2. \end{aligned}$$

Then, we deduce,

$$\|W\|_{a_h^\ell}^2 \leq c\lambda_i \|u_j - \Pi_h u_j\|_{m_h^\ell}^2 + c(1 + \lambda_i) \|W\|_{m_h^\ell}^2 + ch^{2r+1} (\lambda_i^2 + (1 + \lambda_i)^2) \|u_j\|_{\mathbb{H}^2(\Omega, \Gamma)}^2. \quad (5.29)$$

Using the estimation (5.29) in the inequality (5.28), we get,

$$\begin{aligned} \|W\|_{m_h^\ell}^2 &\leq c\mu_J^2 \|u_j - \Pi_h u_j\|_{m_h^\ell}^2 + c\mu_J^2 h^{2r+1} \|u_j\|_{\mathbb{H}^2(\Omega, \Gamma)}^2 + (\epsilon_1^2 + \frac{\epsilon_2^2}{\lambda_i^2}) \|W\|_{a_h^\ell}^2 \\ &\leq c\mu_J^2 \|u_j - \Pi_h u_j\|_{m_h^\ell}^2 + c\mu_J^2 h^{2r+1} \|u_j\|_{\mathbb{H}^2(\Omega, \Gamma)}^2 + c(\epsilon_1^2 + \frac{\epsilon_2^2}{\lambda_i^2}) \lambda_i \|u_j - \Pi_h u_j\|_{m_h^\ell}^2 \\ &\quad + c(\epsilon_1^2 + \frac{\epsilon_2^2}{\lambda_i^2}) (1 + \lambda_i) \|W\|_{m_h^\ell}^2 + ch^{2r+1} (\epsilon_1^2 + \frac{\epsilon_2^2}{\lambda_i^2}) (\lambda_i^2 + (1 + \lambda_i)^2) \|u_j\|_{\mathbb{H}^2(\Omega, \Gamma)}^2 \\ &\leq c\mu_J^2 \|u_j - \Pi_h u_j\|_{m_h^\ell}^2 + c\mu_J^2 h^{2r+1} \|u_j\|_{\mathbb{H}^2(\Omega, \Gamma)}^2 + c(\lambda_i + \frac{1}{\lambda_i}) \|u_j - \Pi_h u_j\|_{m_h^\ell}^2 \\ &\quad + c(\epsilon_1^2 + \frac{\epsilon_2^2}{\lambda_i^2}) (1 + \lambda_i) \|W\|_{m_h^\ell}^2 + ch^{2r+1} (1 + \frac{1}{\lambda_i^2}) (\lambda_i^2 + (1 + \lambda_i)^2) \|u_j\|_{\mathbb{H}^2(\Omega, \Gamma)}^2. \end{aligned}$$

Taking $\epsilon_1 = \frac{1}{2} \sqrt{(\frac{1}{c(1+\lambda_i)})}$ and $\epsilon_2 = \frac{\lambda_i}{2} \sqrt{(\frac{1}{c(1+\lambda_i)})}$, these quantities will satisfy the following inequality,

$$1 - (\epsilon_1^2 + \frac{\epsilon_2^2}{\lambda_i^2}) (1 + \lambda_i) > 0.$$

Then we have,

$$\|W\|_{m_h^\ell}^2 \leq c\lambda_i \|u_j - \Pi_h u_j\|_{m_h^\ell}^2 + c'_{\lambda_i} h^{2r+1} \|u_j\|_{\mathbb{H}^2(\Omega, \Gamma)}^2,$$

where $c_{\lambda_i} = c(\mu_J^2 + \lambda_i + \frac{1}{\lambda_i})$ and $c'_{\lambda_i} = c(\mu_J^2 + (1 + \frac{1}{\lambda_i^2})(\lambda_i^2 + (1 + \lambda_i)^2))$. To arrive to the inequality (5.24), we take the square root of the latter inequality.

3. Lastly we also need to estimate the a_h^ℓ norm of W . We use the estimations (5.29) and (5.24) as follows,

$$\begin{aligned} \|W\|_{a_h^\ell}^2 &\leq c\lambda_i \|u_j - \Pi_h u_j\|_{m_h^\ell}^2 + c(1 + \lambda_i) \|W\|_{m_h^\ell}^2 + ch^{2r+1}(\lambda_i^2 + (1 + \lambda_i)^2) \|u_j\|_{\mathbb{H}^2(\Omega, \Gamma)}^2 \\ &\leq c\lambda_i \|u_j - \Pi_h u_j\|_{m_h^\ell}^2 + c(\lambda_i^2 + (1 + \lambda_i)^2) h^{2r+1} \|u_j\|_{\mathbb{H}^2(\Omega)}^2 \\ &\quad + c(\lambda_i + 1) \left(c\lambda_i \|u_j - \Pi_h u_j\|_{m_h^\ell}^2 + c'_{\lambda_i} h^{2r+1} \|u_j\|_{\mathbb{H}^2(\Omega, \Gamma)}^2 \right). \end{aligned}$$

Consequently we arrive at the desired result by taking its square root,

$$\|W\|_{a_h^\ell} \leq C_{\lambda_i} \|u_j - \Pi_h u_j\|_{m_h^\ell} + C'_{\lambda_i} h^{r+1/2} \|u_j\|_{\mathbb{H}^2(\Omega, \Gamma)},$$

where $C_{\lambda_i} = \sqrt{c(\lambda_i + (\lambda_i + 1)c_{\lambda_i})}$ and $C'_{\lambda_i} = \sqrt{c(\lambda_i^2 + (1 + \lambda_i)^2 + (\lambda_i + 1)c'_{\lambda_i})}$.

□

Remark 5.4. *In this work, the function $W = \Pi_h u_j - \mathcal{P}_{a_h^\ell} u_j$ being a linear combination of lifted discrete eigenfunctions is in the lifted finite element space \mathbb{V}_h^ℓ , which is a subspace of $\mathbb{H}^1(\Omega, \Gamma)$, therefore W is not necessarily in $\mathbb{H}^2(\Omega)$. However if, by considering other finite element method like Hermite, W will be in $\mathbb{H}^2(\Omega, \Gamma)$, then the inequality (5.24) may be improved as follows,*

$$\|W\|_{m_h^\ell}^2 \leq c\lambda_i \|u_j - \Pi_h u_j\|_{m_h^\ell}^2 + c_{\lambda_i} h^{2r+2} \|u_j\|_{\mathbb{H}^2(\Omega, \Gamma)}^2.$$

This may lead to a higher geometric error rate in the final error estimation for the L^2 norm. However, notice that this conjecture should be checked carefully (but this is not the topic of the present paper).

The last step would be to combine all the previous results to estimate the eigenfunctions.

Proof of Theorem 5.1: the estimates (5.2) and (5.3). To prove (5.3), we start by adding and subtracting $\Pi_h u_j$ as follows,

$$\|u_j - \mathcal{P}_{a_h^\ell} u_j\|_{a_h^\ell} \leq \|u_j - \Pi_h u_j\|_{a_h^\ell} + \|\Pi_h u_j - \mathcal{P}_{a_h^\ell} u_j\|_{a_h^\ell} = \|u_j - \Pi_h u_j\|_{a_h^\ell} + \|W\|_{a_h^\ell}.$$

The latter inequality is obtained by definition of $W = \Pi_h u_j - \mathcal{P}_{a_h^\ell} u_j$. Applying respectively (5.25), (5.15) and (5.14), we get,

$$\begin{aligned} \|u_j - \mathcal{P}_{a_h^\ell} u_j\|_{a_h^\ell} &\leq c \|u_j - \Pi_h u_j\|_{a_h^\ell} + C_{\lambda_i} \|u_j - \Pi_h u_j\|_{m_h^\ell} + C'_{\lambda_i} h^{r+1/2} \|u_j\|_{\mathbb{H}^2(\Omega, \Gamma)} \\ &\leq c_{\lambda_i} (h^k + h^{r+1/2}). \end{aligned}$$

By the norm equivalence between $\|\cdot\|_{a_h^\ell}$ and $\|\cdot\|_{\mathbb{H}^1(\Omega, \Gamma)}$, the latter inequality leads to (5.3).

Since $\mathcal{P}_{m_h^\ell}$ is the orthogonal projection with respect to m_h^ℓ onto \mathbb{F}_h^ℓ , then $\mathcal{P}_{m_h^\ell} u_j$ is the closest point to u_j with respect to the m_h^ℓ -norm. Since $\mathcal{P}_{a_h^\ell} = \mathcal{P}_{m_h^\ell} \circ \Pi_h$ as mentioned in Remark 5.3, we have,

$$\|u_j - \mathcal{P}_{m_h^\ell} u_j\|_{m_h^\ell} \leq \|u_j - \mathcal{P}_{a_h^\ell} u_j\|_{m_h^\ell} \leq \|u_j - \Pi_h u_j\|_{m_h^\ell} + \|\Pi_h u_j - \mathcal{P}_{a_h^\ell} u_j\|_{m_h^\ell}.$$

We apply (5.24) and (5.15) respectively to conclude,

$$\|u_j - \mathcal{P}_{m_h^\ell} u_j\|_{m_h^\ell} \leq c_{\lambda_i} \|u_j - \Pi_h u_j\|_{m_h^\ell} + c'_{\lambda_i} h^{r+1/2} \|u_j\|_{\mathbb{H}^2(\Omega, \Gamma)} \leq c_{\lambda_i} (h^{k+1} + h^{r+1/2}).$$

By the norm equivalence between $\|\cdot\|_{m_h^\ell}$ and $\|\cdot\|_{L^2(\Omega)}$, the latter inequality leads to (5.2).

5.4 Eigenvalue error estimate

We recall that λ_i is an exact eigenvalue of multiplicity N of Problem (2.1), such that $\lambda_j = \lambda_i$, for any $j \in J = \{i, \dots, i + N - 1\}$. In order to improve the preliminary eigenvalue error estimation (5.9), we introduce $\mathcal{P}_m : \mathbb{V}_h^\ell \rightarrow \mathbb{E}_{\lambda_i}$ the orthogonal projection with respect to m onto the space \mathbb{E}_{λ_i} , such that for all $v \in \mathbb{V}_h^\ell$,

$$m(\mathcal{P}_m v, t) = m(v, t), \quad \forall t \in \mathbb{E}_{\lambda_i}.$$

The idea of the following lemma can be found in [2, Lemma 2.3] and [3, Lemma 3.1]. However the main difference here is that we need to take into consideration the geometric error (see [6, Lemma 6.1] and [4, Lemma 5.1]).

Lemma 5.1 (eigenvalue bound). *Let U_j^ℓ be a discrete eigenfunction in \mathbb{F}_h^ℓ associated to Λ_j such that $\|U_j^\ell\|_m = 1$. Thus, the following inequality holds,*

$$|\lambda_j - \Lambda_j| \leq \|\mathcal{P}_m U_j^\ell - U_j^\ell\|_a^2 + \lambda_j \|\mathcal{P}_m U_j^\ell - U_j^\ell\|_m^2 + |a_h^\ell - a|(U_j^\ell, U_j^\ell) + \Lambda_j |m_h^\ell - m|(U_j^\ell, U_j^\ell). \quad (5.30)$$

Proof. First of all, we need to notice that $\mathcal{P}_m U_j^\ell$ is in \mathbb{E}_{λ_i} , thus,

$$a(\mathcal{P}_m U_j^\ell, v) = \lambda_j m(\mathcal{P}_m U_j^\ell, v), \quad \forall v \in H^1(\Omega, \Gamma). \quad (5.31)$$

Taking $v = U_j^\ell \in H^1(\Omega, \Gamma)$ in (5.31), we have,

$$a(\mathcal{P}_m U_j^\ell, U_j^\ell) = \lambda_j m(\mathcal{P}_m U_j^\ell, U_j^\ell).$$

Afterwards, taking $v = \mathcal{P}_m U_j^\ell \in H^1(\Omega, \Gamma)$ in (5.31), we get,

$$\|\mathcal{P}_m U_j^\ell\|_a^2 = \lambda_j \|\mathcal{P}_m U_j^\ell\|_m^2.$$

Applying the latter two equations in the following estimation, we get,

$$\begin{aligned} & \|\mathcal{P}_m U_j^\ell - U_j^\ell\|_a^2 - \lambda_j \|\mathcal{P}_m U_j^\ell - U_j^\ell\|_m^2 \\ &= \|\mathcal{P}_m U_j^\ell\|_a^2 + \|U_j^\ell\|_a^2 - 2a(U_j^\ell, \mathcal{P}_m U_j^\ell) - \lambda_j \|U_j^\ell\|_m^2 - \lambda_j \|\mathcal{P}_m U_j^\ell\|_m^2 + 2\lambda_j m(U_j^\ell, \mathcal{P}_m U_j^\ell) \\ &= \|U_j^\ell\|_a^2 - \lambda_j \|U_j^\ell\|_m^2. \end{aligned}$$

Since $\|U_j^\ell\|_m = 1$, we have,

$$-\lambda_j = \|\mathcal{P}_m U_j^\ell - U_j^\ell\|_a^2 - \lambda_j \|\mathcal{P}_m U_j^\ell - U_j^\ell\|_m^2 - \|U_j^\ell\|_a^2.$$

Keeping in mind that $a_h^\ell(U_j^\ell, U_j^\ell) = \Lambda_j m_h^\ell(U_j^\ell, U_j^\ell)$, we get by adding and subtracting $a_h^\ell(U_j^\ell, U_j^\ell)$,

$$\begin{aligned} -\lambda_j &= \|\mathcal{P}_m U_j^\ell - U_j^\ell\|_a^2 - \lambda_j \|\mathcal{P}_m U_j^\ell - U_j^\ell\|_m^2 - a(U_j^\ell, U_j^\ell) + a_h^\ell(U_j^\ell, U_j^\ell) - \Lambda_j m_h^\ell(U_j^\ell, U_j^\ell) \\ &= \|\mathcal{P}_m U_j^\ell - U_j^\ell\|_a^2 - \lambda_j \|\mathcal{P}_m U_j^\ell - U_j^\ell\|_m^2 + (a_h^\ell - a)(U_j^\ell, U_j^\ell) - \Lambda_j m_h^\ell(U_j^\ell, U_j^\ell). \end{aligned}$$

Since $m(U_j^\ell, U_j^\ell) = 1$, then by adding $\Lambda_j m(U_j^\ell, U_j^\ell)$ to each side of this equation, we have,

$$\Lambda_j - \lambda_j = \|\mathcal{P}_m U_j^\ell - U_j^\ell\|_a^2 - \lambda_j \|\mathcal{P}_m U_j^\ell - U_j^\ell\|_m^2 + (a_h^\ell - a)(U_j^\ell, U_j^\ell) + \Lambda_j (m - m_h^\ell)(U_j^\ell, U_j^\ell).$$

By taking the absolute value of the latter equation and bounding it, we get (5.30). \square

The proofs of the following lemma and corollary are analogous to the proofs of [6, Lemma 4.4 - Proposition 4.5], which were given for a surface problem. For readers convenience, we will detail these proofs, and we recall that there exists $c_{\lambda_i} > 0$, such that $0 < \Lambda_j \leq c_{\lambda_i}$, for all $j \in \mathbf{J}$.

Lemma 5.2. *Following the assumption in Lemma 5.1, there exists $c_{\lambda_i} > 0$ such that,*

$$\|\mathcal{P}_{m_h^\ell} v\|_{a_h^\ell} \leq c_{\lambda_i} \|v\|_{m_h^\ell}, \quad \forall v \in \mathbf{H}^1(\Omega, \Gamma), \quad (5.32)$$

where $\mathcal{P}_{m_h^\ell}$ is the orthogonal projection with respect to m_h^ℓ onto \mathbb{F}_h^ℓ , given in Definition 5.1.

Proof. Notice that $\mathcal{P}_{m_h^\ell} v \in \mathbb{F}_h^\ell = \bigoplus_{j \in \mathbf{J}} \mathbb{E}_{\Lambda_j}^\ell$, then there exists constants $\beta_j \in \mathbb{R}$ for $j \in \mathbf{J}$ such that $\mathcal{P}_{m_h^\ell} v = \sum_{j \in \mathbf{J}} \beta_j U_j^\ell$. One can estimate its norm as follows,

$$\begin{aligned} \|\mathcal{P}_{m_h^\ell} v\|_{a_h^\ell}^2 &= a_h^\ell(\mathcal{P}_{m_h^\ell} v, \mathcal{P}_{m_h^\ell} v) = a_h^\ell\left(\sum_{j \in \mathbf{J}} \beta_j U_j^\ell, \mathcal{P}_{m_h^\ell} v\right) \\ &= \sum_{j \in \mathbf{J}} \beta_j a_h^\ell(U_j^\ell, \mathcal{P}_{m_h^\ell} v) = \sum_{j \in \mathbf{J}} \beta_j \Lambda_j m_h^\ell(U_j^\ell, \mathcal{P}_{m_h^\ell} v). \end{aligned}$$

Since $0 < \Lambda_j \leq c_{\lambda_i}$, for all $j \in \mathbf{J}$, we have,

$$\|\mathcal{P}_{m_h^\ell} v\|_{a_h^\ell}^2 \leq c_{\lambda_i} \sum_{j \in \mathbf{J}} \beta_j m_h^\ell(U_j^\ell, \mathcal{P}_{m_h^\ell} v) = c_{\lambda_i} m_h^\ell(\mathcal{P}_{m_h^\ell} v, \mathcal{P}_{m_h^\ell} v) = c_{\lambda_i} \|\mathcal{P}_{m_h^\ell} v\|_{m_h^\ell}^2.$$

Finally, by definition of the orthogonal projection $\mathcal{P}_{m_h^\ell}$, we conclude the proof as follows,

$$\|\mathcal{P}_{m_h^\ell} v\|_{a_h^\ell}^2 \leq c_{\lambda_i} \|v\|_{m_h^\ell}^2. \quad \square$$

Corollary 5.3. *Following the assumptions of lemma 5.2, this inequality holds for any exact eigenfunction u_j associated to λ_i , there exists $c_{\lambda_i} > 0$ such that,*

$$\|u_j - \mathcal{P}_{m_h^\ell} u_j\|_{a_h^\ell} \leq \|u_j - \mathcal{P}_{a_h^\ell} u_j\|_{a_h^\ell} + c_{\lambda_i} \|u_j - \Pi_h u_j\|_{m_h^\ell}, \quad (5.33)$$

where Π_h is the orthogonal projection with respect to a_h^ℓ onto \mathbb{V}_h^ℓ and $\mathcal{P}_{a_h^\ell}$ is the orthogonal projection with respect to a_h^ℓ onto \mathbb{F}_h^ℓ , given in Definition 5.1.

Proof. By adding and subtracting $\mathcal{P}_{a_h^\ell} u_j$, we have,

$$\|u_j - \mathcal{P}_{m_h^\ell} u_j\|_{a_h^\ell} \leq \|u_j - \mathcal{P}_{a_h^\ell} u_j\|_{a_h^\ell} + \|\mathcal{P}_{a_h^\ell} u_j - \mathcal{P}_{m_h^\ell} u_j\|_{a_h^\ell}.$$

Since $\mathcal{P}_{a_h^\ell} = \mathcal{P}_{m_h^\ell} \circ \Pi_h$, we get,

$$\begin{aligned} \|u_j - \mathcal{P}_{m_h^\ell} u_j\|_{a_h^\ell} &\leq \|u_j - \mathcal{P}_{a_h^\ell} u_j\|_{a_h^\ell} + \|\mathcal{P}_{m_h^\ell} \circ \Pi_h u_j - \mathcal{P}_{m_h^\ell} u_j\|_{a_h^\ell} \\ &= \|u_j - \mathcal{P}_{a_h^\ell} u_j\|_{a_h^\ell} + \|\mathcal{P}_{m_h^\ell} (\Pi_h u_j - u_j)\|_{a_h^\ell}. \end{aligned}$$

To sum up, we apply (5.32) to arrive at (5.33). \square

The error between a discrete eigenfunction and its projection onto the space spanned by the exact eigenfunctions is estimated in the following lemmas using \mathcal{P}_m the orthogonal projection with respect to m onto the space \mathbb{E}_{λ_i} .

By [22, Lemma 5.1], for a sufficiently small h , $\{\mathcal{P}_{m_h^\ell} u_p, p \in \mathbb{J}\}$ forms a basis for \mathbb{F}_h^ℓ . Since $U_j^\ell \in \mathbb{F}_h^\ell = \text{span}\{\mathcal{P}_{m_h^\ell} u_p, p \in \mathbb{J}\}$, it can be written as follows,

$$U_j^\ell = \sum_{p \in \mathbb{J}} \alpha_p \mathcal{P}_{m_h^\ell} u_p. \quad (5.34)$$

Indeed, this can be traced back to the lower semicontinuity of the rank application and the fact that $\mathcal{P}_{m_h^\ell} u_p$ tends to u_p as h tends to 0, for all $p \in \mathbb{J}$.

Lemma 5.3. *Let U_j be a discrete eigenfunction associated to Λ_j , such that $\|U_j^\ell\|_m = 1$. Then, we have,*

$$\mathcal{P}_m U_j^\ell - U_j^\ell = \sum_{p \in \mathbb{J}} \alpha_p \left[\sum_{t \in \mathbb{J}} m(\mathcal{P}_{m_h^\ell} u_p - u_p, u_t) u_t + (u_p - \mathcal{P}_{m_h^\ell} u_p) \right], \quad (5.35)$$

where $\{u_p\}_{p \in \mathbb{J}}$ denotes an orthonormal basis of \mathbb{E}_{λ_i} with respect to m (thus made of exact eigenfunctions associated to λ_i).

Proof. We will proceed as in [6, lem 6.2 - 6.3]. We need to keep in mind that \mathcal{P}_m is the orthogonal projection with respect to m on \mathbb{E}_{λ_i} . This implies that $\mathcal{P}_m U_j^\ell$ can be written as follows,

$$\mathcal{P}_m U_j^\ell = \sum_{t \in \mathbb{J}} m(U_j^\ell, u_t) u_t \in \mathbb{E}_{\lambda_i}. \quad (5.36)$$

Subtracting (5.34) from the latter equation (5.36), we get,

$$\mathcal{P}_m U_j^\ell - U_j^\ell = \sum_{t \in \mathbb{J}} m\left(\sum_{p \in \mathbb{J}} \alpha_p \mathcal{P}_{m_h^\ell} u_p, u_t\right) u_t - \sum_{p \in \mathbb{J}} \alpha_p \mathcal{P}_{m_h^\ell} u_p. \quad (5.37)$$

Since $m(u_p, u_t) = \delta_{pt}$ for all $p, t \in \mathbb{J}$, we have,

$$-\sum_{p \in \mathbb{J}} \alpha_p m(u_p, u_p) u_p + \sum_{p \in \mathbb{J}} \alpha_p u_p = 0.$$

Inserting this in (5.37), we get,

$$\begin{aligned} \mathcal{P}_m U_j^\ell - U_j^\ell &= \sum_{t \in \mathbb{J}} m\left(\sum_{p \in \mathbb{J}} \alpha_p \mathcal{P}_{m_h^\ell} u_p, u_t\right) u_t - \sum_{p \in \mathbb{J}} \alpha_p m(u_p, u_p) u_p + \sum_{p \in \mathbb{J}} \alpha_p (u_p - \mathcal{P}_{m_h^\ell} u_p) \\ &= \sum_{t \in \mathbb{J}} \sum_{p \in \mathbb{J}} \alpha_p m(\mathcal{P}_{m_h^\ell} u_p - u_p, u_t) u_t + \sum_{p \in \mathbb{J}} \alpha_p (u_p - \mathcal{P}_{m_h^\ell} u_p) \\ &= \sum_{p \in \mathbb{J}} \alpha_p \left[\sum_{t \in \mathbb{J}} m(\mathcal{P}_{m_h^\ell} u_p - u_p, u_t) u_t + (u_p - \mathcal{P}_{m_h^\ell} u_p) \right]. \end{aligned}$$

□

Lemma 5.4. *Let U_j be an eigenfunction associated to Λ_j such that $\|U_j^\ell\|_m = 1$. Then, for a sufficiently small mesh size h , there exists $c_{\lambda_i} > 0$ such that,*

$$\|U_j^\ell - \mathcal{P}_m U_j^\ell\|_a \leq c_{\lambda_i} \max_{p \in \mathbb{J}} \|u_p - \mathcal{P}_{m_h^\ell} u_p\|_a, \quad (5.38)$$

$$\|U_j^\ell - \mathcal{P}_m U_j^\ell\|_m \leq c_{\lambda_i} \max_{p \in \mathbb{J}} \|u_p - \mathcal{P}_{m_h^\ell} u_p\|_m, \quad (5.39)$$

$$\|U_j^\ell - \mathcal{P}_m U_j^\ell\|_a \leq c_{\lambda_i} (h^k + h^{r+1/2}), \quad (5.40)$$

$$\|U_j^\ell - \mathcal{P}_m U_j^\ell\|_m \leq c_{\lambda_i} (h^{k+1} + h^{r+1/2}). \quad (5.41)$$

where $\mathcal{P}_{m_h^\ell}$ is the orthogonal projection over \mathbb{F}_h^ℓ with respect to m_h^ℓ , given in Definition 5.1.

Proof. Taking the norm with respect to the bilinear form a of (5.35), we bound it as follows,

$$\|\mathcal{P}_m U_j^\ell - U_j^\ell\|_a \leq \sum_{p \in \mathbf{J}} |\alpha_p| \left[\sum_{t \in \mathbf{J}} |m(\mathcal{P}_{m_h^\ell} u_p - u_p, u_t)| \|u_t\|_a + \|u_p - \mathcal{P}_{m_h^\ell} u_p\|_a \right].$$

By applying Cauchy-Schwarz, we have,

$$\|\mathcal{P}_m U_j^\ell - U_j^\ell\|_a \leq \left(\sum_{p \in \mathbf{J}} |\alpha_p|^2 \right)^{\frac{1}{2}} \left(\sum_{p \in \mathbf{J}} \left[\sum_{t \in \mathbf{J}} |m(\mathcal{P}_{m_h^\ell} u_p - u_p, u_t)| \|u_t\|_a + \|u_p - \mathcal{P}_{m_h^\ell} u_p\|_a \right]^2 \right)^{\frac{1}{2}}.$$

By Lemma 5.1 of [22] the coefficients $(\alpha_p)_{p \in \mathbf{J}}$ satisfy, $\sum_{p \in \mathbf{J}} |\alpha_p|^2 \leq C(N)$, where $C(N)$ is a constant dependent on the multiplicity N of λ_i . Keeping in mind that, for all $t \in \mathbf{J}$, u_t satisfies that, $a(u_t, v) = \lambda_i m(u_t, v)$, for any $v \in H^1(\Omega, \Gamma)$, we have,

$$\begin{aligned} \|\mathcal{P}_m U_j^\ell - U_j^\ell\|_a &\leq (C(N))^{\frac{1}{2}} \left(\sum_{p \in \mathbf{J}} \left[\sum_{t \in \mathbf{J}} \frac{1}{\lambda_i} |a(\mathcal{P}_{m_h^\ell} u_p - u_p, u_t)| \|u_t\|_a + \|u_p - \mathcal{P}_{m_h^\ell} u_p\|_a \right]^2 \right)^{\frac{1}{2}} \\ &\leq c_{\lambda_i} \left(\sum_{p \in \mathbf{J}} \left[\sum_{t \in \mathbf{J}} \frac{1}{\lambda_i} \|\mathcal{P}_{m_h^\ell} u_p - u_p\|_a \|u_t\|_a \|u_t\|_a + \|u_p - \mathcal{P}_{m_h^\ell} u_p\|_a \right]^2 \right)^{\frac{1}{2}} \\ &\leq c_{\lambda_i} \left(\sum_{p \in \mathbf{J}} \left[\sum_{t \in \mathbf{J}} \|\mathcal{P}_{m_h^\ell} u_p - u_p\|_a \frac{1}{\lambda_i} \|u_t\|_a^2 + \|u_p - \mathcal{P}_{m_h^\ell} u_p\|_a \right]^2 \right)^{\frac{1}{2}}. \end{aligned}$$

Noticing that $\frac{1}{\lambda_i} \|u_t\|_a^2 = \|u_t\|_m^2 = 1$ for all $t \in \mathbf{J}$, we have,

$$\|\mathcal{P}_m U_j^\ell - U_j^\ell\|_a \leq c_{\lambda_i} \left(\sum_{p \in \mathbf{J}} \left[\sum_{t \in \mathbf{J}} 2 \|\mathcal{P}_{m_h^\ell} u_p - u_p\|_a \right]^2 \right)^{\frac{1}{2}}.$$

Then, we arrive at the inequality (5.38) given by,

$$\|\mathcal{P}_m U_j^\ell - U_j^\ell\|_a \leq c_{\lambda_i} \max_{p \in \mathbf{J}} \|u_p - \mathcal{P}_{m_h^\ell} u_p\|_a.$$

To prove (5.40), we need to keep in mind that the norms with respect to the bilinear forms a and a_h^ℓ are equivalent and we use (5.33) as follows,

$$\|u_p - \mathcal{P}_{m_h^\ell} u_p\|_a \leq c \|u_p - \mathcal{P}_{m_h^\ell} u_p\|_{a_h^\ell} \leq c \|u_p - \mathcal{P}_{a_h^\ell} u_p\|_{a_h^\ell} + c_{\lambda_i} \|u_p - \Pi_h u_p\|_{m_h^\ell}.$$

By applying again the norm equivalence and using the error estimations (5.3) and (5.15), we have,

$$\|u_p - \mathcal{P}_{m_h^\ell} u_p\|_a \leq c_{\lambda_i} (h^k + h^{r+1/2}).$$

Combining the latter inequality with (5.38), we obtain (5.40).

Passing to the proof of Inequality (5.39), we consider the norm with respect to m of (5.35) as follows,

$$\|\mathcal{P}_m U_j^\ell - U_j^\ell\|_m \leq \sum_{p \in J} |\alpha_p| \left[\sum_{t \in J} |m(\mathcal{P}_{m_h^\ell} u_p - u_p, u_t)| \|u_t\|_m + \|u_p - \mathcal{P}_{m_h^\ell} u_p\|_m \right]$$

Using Cauchy-Schwarz, we proceed in a similar manner as for the previous inequality,

$$\begin{aligned} \|\mathcal{P}_m U_j^\ell - U_j^\ell\|_m &\leq \left(\sum_{p \in J} |\alpha_p|^2 \right)^{\frac{1}{2}} \left(\sum_{p \in J} \left[\sum_{t \in J} |m(\mathcal{P}_{m_h^\ell} u_p - u_p, u_t)| \|u_t\|_m + \|u_p - \mathcal{P}_{m_h^\ell} u_p\|_m \right]^2 \right)^{\frac{1}{2}} \\ &\leq (C(N))^{\frac{1}{2}} \left(\sum_{p \in J} \left[\sum_{t \in J} \|\mathcal{P}_{m_h^\ell} u_p - u_p\|_m \|u_t\|_m \|u_t\|_m + \|u_p - \mathcal{P}_{m_h^\ell} u_p\|_m \right]^2 \right)^{\frac{1}{2}} \\ &\leq c_{\lambda_i} \left(\sum_{p \in J} \left[\sum_{t \in J} 2 \|\mathcal{P}_{m_h^\ell} u_p - u_p\|_m \right]^2 \right)^{\frac{1}{2}}, \end{aligned}$$

where we used $\|u_t\|_m^2 = 1$. Consequently, we obtain the inequality (5.39). Lastly, using the error estimation (5.2), we obtain (5.41). \square

Proof of Theorem 5.1: the eigenvalue estimation (5.1). Firstly we recall (5.30), we get,

$$|\lambda_j - \Lambda_j| \leq \|\mathcal{P}_m U_j^\ell - U_j^\ell\|_a^2 + \lambda_j \|\mathcal{P}_m U_j^\ell - U_j^\ell\|_m^2 + |a_h^\ell - a|(U_j^\ell, U_j^\ell) + \Lambda_j |m_h^\ell - m|(U_j^\ell, U_j^\ell).$$

Secondly, we use (5.40), (5.41) and (5.8) to arrive at,

$$\begin{aligned} |\lambda_j - \Lambda_j| &\leq c_{\lambda_i} (h^{2k} + h^{2r+1}) + \lambda_j c_{\lambda_i} (h^{2k+2} + h^{2r+1}) + |a_h^\ell - a|(U_j^\ell, U_j^\ell) + c_{\Lambda_j} h^{r+1} \|U_j^\ell\|_{\mathbb{H}^1(\Omega, \Gamma)}^2 \\ &\leq c_{\lambda_i} (h^{2k} + h^{2r+1}) + |a_h^\ell - a|(U_j^\ell, U_j^\ell) + c_{\Lambda_j} h^{r+1} \|U_j^\ell\|_{\mathbb{H}^1(\Omega, \Gamma)}^2. \end{aligned}$$

The remaining term can be estimated as such by using (5.7),

$$|a_h^\ell - a|(U_j^\ell, U_j^\ell) \leq ch^r \|\nabla U_j^\ell\|_{L^2(B_h^\ell)}^2 + ch^{r+1} \|U_j^\ell\|_{\mathbb{H}^1(\Gamma)}^2$$

By adding and subtraction $\mathcal{P}_m U_j^\ell$ as follow, and then applying (5.40), we get,

$$\begin{aligned} |a_h^\ell - a|(U_j^\ell, U_j^\ell) &\leq ch^r \|\nabla(\mathcal{P}_m U_j^\ell - U_j^\ell)\|_{L^2(B_h^\ell)}^2 + ch^r \|\nabla(\mathcal{P}_m U_j^\ell)\|_{L^2(B_h^\ell)}^2 + ch^{r+1} \|U_j^\ell\|_{\mathbb{H}^1(\Gamma)}^2 \\ &\leq c_{\lambda_i} h^r (h^{2k} + h^{2r+1}) + ch^r \|\nabla(\mathcal{P}_m U_j^\ell)\|_{L^2(B_h^\ell)}^2 + ch^{r+1} \|U_j^\ell\|_{\mathbb{H}^1(\Gamma)}^2 \\ &\leq c_{\lambda_i} (h^{2k+r} + h^{3r+1}) + ch^r \|\nabla(\mathcal{P}_m U_j^\ell)\|_{L^2(B_h^\ell)}^2 + ch^{r+1} \|U_j^\ell\|_{\mathbb{H}^1(\Gamma)}^2. \end{aligned}$$

Since we have $\mathcal{P}_m U_j^\ell \in \mathbb{E}_{\lambda_i}$ a linear combination of exacts eigenvalues, then $\mathcal{P}_m U_j^\ell \in \mathbb{H}^2(\Omega, \Gamma)$ and the inequality (5.5) can be applied to it as follows,

$$\begin{aligned} |a_h^\ell - a|(U_j^\ell, U_j^\ell) &\leq c_{\lambda_i} (h^{2k+r} + h^{3r+1}) + ch^r (h^{1/2} \|\mathcal{P}_m U_j^\ell\|_{\mathbb{H}^2(\Omega)})^2 + ch^{r+1} \|U_j^\ell\|_{\mathbb{H}^1(\Gamma)}^2 \\ &\leq c_{\lambda_i} (h^{2k+r} + h^{3r+1}) + ch^{r+1} \|\mathcal{P}_m U_j^\ell\|_{\mathbb{H}^2(\Omega)}^2 + ch^{r+1} \|U_j^\ell\|_{\mathbb{H}^1(\Gamma)}^2 \\ &\leq c_{\lambda_i} h^{r+1} (\|\mathcal{P}_m U_j^\ell\|_{\mathbb{H}^2(\Omega)}^2 + \|U_j^\ell\|_{\mathbb{H}^1(\Gamma)}^2), \end{aligned}$$

where $\|\mathcal{P}_m U_j^\ell\|_{\mathbb{H}^2(\Omega)}^2 + \|U_j^\ell\|_{\mathbb{H}^1(\Gamma)}^2$ is uniformly bounded with respect to h and r . Since the exact eigenfunctions are sufficiently regular and we supposed that $\|U_j^\ell\|_{L^2(\Omega)} = \|u_t\|_{L^2(\Omega)} = 1$, by (5.36), $\|\mathcal{P}_m U_j^\ell\|_{\mathbb{H}^2(\Omega)}$ is bounded independently of h . By Inequality (5.40), $\text{dist}(U_j^\ell, \mathbb{E}_{\lambda_i}) \rightarrow 0$ where \mathbb{E}_{λ_i} is of finite dimension, we can bound $\|U_j^\ell\|_{\mathbb{H}^1(\Gamma)}$ independently of h . Finally, replacing this inequality in the eigenvalue estimation, we get the desired result (5.1).

6 Numerical experiments

In this section are presented numerical results aimed to illustrate the convergence estimates of Theorem 5.1. We perform these simulations in the two dimensional and three dimensional cases. The Ventcel problem (1.1) is considered on various domains. The discrete problem (4.1) is implemented and solved using the finite element library CUMIN [31]. The resolution of the spectral problem is done with the help of the library ARPACK², which is a numerical software library for solving large scale eigenvalue problems. The symmetric case (the iterative Lanczos algorithm) is used in shift invert mode with a shift value $\sigma = -1$ (in order to accurately compute the eigenvalues of smallest amplitude). For this method, linear systems $Ax = b$ have to be solved for a single matrix A and for numerous varying right hand sides: a linear system solver is required for the sparse CSR matrix A that is symmetric and positive definite.

In dimension 2, the direct solver MUMPS³ (Multifrontal Massively Parallel sparse direct Solver) is considered allowing fast computations. It is particularly well adapted in the present context where linear systems involving the same matrix A have to be solved many times. Cholesky LL^T decomposition of a single (positive definite) CSR sparse matrix is computed once at the beginning and afterwards used for numerous linear equation resolutions all along the spectral Lanczos algorithm. The tolerance for the Lanczos algorithm was set to a low value (1E-12): this allowed to compute quickly, while using MUMPS, the numerical errors up to error values of 1E-11, allowing us to study the convergence asymptotic regimes. More details on the computational efforts are given in the following paragraph devoted to the unit disk case.

In dimension 3, memory requirements imposed a lighter method: a conjugate gradient with Jacobi preconditioning has been used. The tolerances for the iterative algorithms (Lanczos and conjugate gradient) have been set to very low values (1E-14): this generally allowed to compute accurately the numerical errors up to error values of 1E-10, which was necessary in order to well capture the convergence asymptotic regimes. The 3D computations are the most demanding in terms of computational effort and time. Therefore, they deserved a specific attention, which is given in the paragraph dealing with the unit ball.

Curved meshes of the domain Ω of geometrical order $1 \leq r \leq 3$ have been generated using the software Gmsh⁴. All integral computations (either on the physical domain Ω or on the computational domain Ω_h^r) are performed on the reference simplex using changes of coordinates. These changes of coordinates are made on each element of the underlying mesh that is considered: either an affine mesh $\mathcal{T}_h^{(1)}$, a curved mesh $\mathcal{T}_h^{(r)}$ or an exact mesh $\mathcal{T}_h^{(e)}$. This allows to compute numerical errors such as $\|u_h^\ell - u\|_{L^2(\Omega)}$ between the lift u_h^ℓ of a finite element function u_h defined on $\Omega_h^{(r)}$ and a function u defined on the smooth domain Ω . On the reference simplex, high order quadrature methods are used such that the integration error is of lower order than the approximation errors that are evaluated in this section: it has systematically been verified that the integration errors have negligible influence over the forthcoming numerical results.

Convergence towards the eigenfunctions has only been studied on domains where the analytical solutions are known (the disk and the ball). On domains where the eigenfunctions are not analytically known, such a convergence study is much more complicated to handle. We would need to compute reference eigenfunctions on a refined reference grid and also to project the numerical solutions defined on coarser meshes. However, in the context of curved meshes, this would lead to non trivial difficulties, which cannot be considered in the present work.

All numerical results presented in this section can be fully reproduced using dedicated source

²<https://www.arpack.fr/>

³<https://mumps-solver.org/index.php>

⁴<https://gmsh.info/>

codes available on CUMIN Gitlab⁵.

6.1 The two dimensional case

Eigenvalue estimate on a smooth domain. The Ventcel problem (1.1) is considered on a smooth domain defined as the interior of a Jordan curve, denoted γ . The curve γ has been set in such a way to have a smooth and connex domain, which moreover is non-convex with no symmetries, in order to avoid eventual *super convergence* properties. Indeed, the domain Ω is the interior of the Jordan curve $\gamma : \theta \in [0, 2\pi] \rightarrow \gamma(\theta) \in \mathbb{R}^2$ satisfying $\gamma(0) = \gamma(2\pi)$. For any $\theta \in [0, 2\pi]$, the function gamma is given by,

$$\gamma(\theta) = (\kappa(\theta) \cos \theta, \kappa(\theta) \sin \theta),$$

where $k(\theta) = 1 + \alpha \cos \theta + \beta \sin \theta + \frac{\beta}{2} \sin 3\theta$, with $\alpha = 0.3$ and $\beta = 0.4$. Curved meshes of order $r = 1, \dots, 3$ are generated using CUMIN and Gmsh (see Figure 1 for linear and quadratic meshes). \mathbb{P}^k finite element methods, with degrees $k = 1, \dots, 4$, are employed to estimate the eigenvalue error.

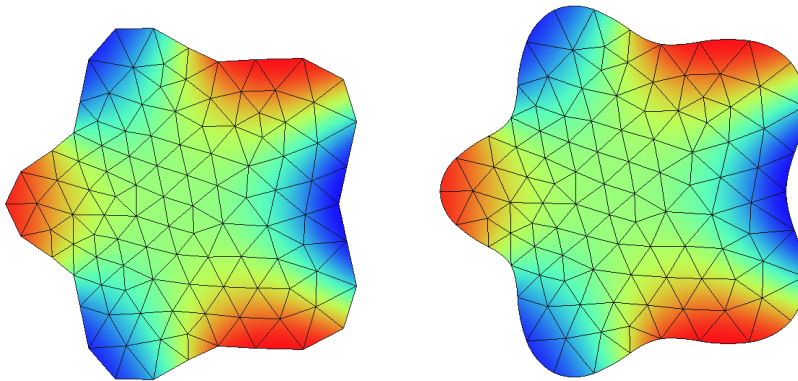


Figure 1: Representation of the 6th eigenfunction computed using \mathbb{P}^3 finite element on a (coarse) mesh of Ω : affine mesh (left) and quadratic mesh (right).

The mesh degree and the finite element order being fixed, the 10 first eigenvalues are computed on a series of successively refined meshes: each mesh counts $20 \times 2^{n-1}$ edges on the domain boundary, for $n = 1, \dots, 5$. We do not know the exact eigenvalues of the Ventcel problem (1.1) on this domain. Thus, reference eigenvalues have been computed on a reference mesh of order $r = 3$ using a \mathbb{P}^4 finite element method. The reference mesh counts 20×2^5 boundary edges and is made of approximately 76 000 cubic triangles, the associated \mathbb{P}^4 finite element space has approximately 610 000 DOF (Degrees Of Freedom). We mention that the computation time is very fast in the present case: total computations roughly last one minute on a simple laptop, which are made really efficient with the direct solver MUMPS here.

To calculate the eigenvalue error, we estimate the difference between the reference eigenvalues, denoted λ_j , and the computed eigenvalues denoted Λ_j . In Table 1, the convergence order of the error associated to the 6th eigenvalue, given by $e_{\lambda_6} := |\lambda_6 - \Lambda_6|$, is presented. We mention that any other choice within the 10 eigenvalues that have been computed lead to the same convergence

⁵Cumin GitLab deposit, <https://plmlab.math.cnrs.fr/cpierre1/cumin>

pattern. The convergence orders are evaluated from the error ratio between two successive meshes. The order estimations display very stable behaviour (no oscillation): we reported in Table 1 the convergence orders estimated between the two finest meshes.

Mesh type	e_{λ_6}			
	\mathbb{P}^1	\mathbb{P}^2	\mathbb{P}^3	\mathbb{P}^4
Affine ($r=1$)	1.96	2.00	2.00	2.00
Quadratic ($r=2$)	1.99	3.97	3.98	3.97
Cubic ($r=3$)	1.99	2.99	4.07	4.08

Table 1: Convergence order of e_{λ_6} (Figures in red represent a loss in the convergence rate).

As displayed in Table 1, the convergence rate of e_{λ_6} on an affine mesh ($r = 1$) are equal to $r + 1 = 2$ for any \mathbb{P}^k finite element method used as expected by the theory.

For the quadratic case ($r = 2$), a *super convergence* is observed: a saturation of the error occurs at order 4 when it was expected to stop at 3. This super convergence had already been observed in [10], [9] and [6]: quadratic meshes seem to behave as if $r = 3$, however no theoretical explanation of this phenomenon has been proposed so far to the authors' knowledge. It is interesting to notice that this super convergence also occurs in the present example though the domain is neither convex nor symmetric. This implies that this phenomenon is not related to some particular geometric properties of the domain, as one might presume.

On the cubic meshes ($r = 3$), the convergence order of e_{λ_6} follows the expected estimate (5.1) and a saturation of the error is observed at order $r + 1 = 4$. The only odd case worth mentioning is when using a \mathbb{P}^2 finite element method on a cubic mesh. In this particular case, we obtained a convergence order of 3 whereas the theory predicts a convergence order of 4. This loss is observed in all the numerical experiments throughout this work and it will be discussed in details in the following paragraph.

Error estimates on the unit disk The Ventcel problem (1.1) is considered on the unit disk $D(O, 1) \subset \mathbb{R}^2$. In this case, the eigenfunctions are the harmonic polynomials. A convergence analysis is performed on the 6th eigenvalue λ_6 of multiplicity 2 with corresponding eigenspace, denoted E_3 , equal to the space of harmonic polynomials of degree 3.

To proceed, \mathbb{P}^k finite element methods, of degrees $k = 1, \dots, 4$, are used for the error estimates on meshes of order $r = 1, \dots, 3$ (see Figure 2 for linear and quadratic meshes). The mesh order and the finite element degree being fixed, the 12 first eigenvalues are computed on a series of five successively refined meshes: each mesh counts $20 \times 2^{n-1}$ edges on the domain boundary, for $n = 1, \dots, 6$. On the most refined mesh using a \mathbb{P}^4 finite element method, we counted 20×2^5 boundary edges and approximately 75 500 triangles. The associated \mathbb{P}^4 finite element space has approximately 605 600 DOF. The computations are accomplished very quickly, the total computation time is less than four minutes on a regular computer.

We denote Λ_6 a numerical eigenvalue approximating λ_6 with U_6 as its associated computed eigenfunction. For each mesh order r and each finite element degree k , the following numerical errors are computed on a series of refined meshes:

$$e_{L^2} := \inf \{ \|U_6^\ell - u\|_{L^2(\Omega)}, u \in E_3 \}, \quad e_{H_0^1} := \inf \{ \|\nabla(U_6^\ell - u)\|_{L^2(\Omega)}, u \in E_3 \},$$

$$\text{and} \quad e_{\lambda_6} := |\lambda_6 - \Lambda_6|.$$

The L^2 distance between U_6^ℓ and the eigenspace E_3 , denoted e_{L^2} , is computed using the L^2 orthogonal projection of U_6^ℓ onto E_3 . In a similar manner, the L^2 distance between ∇U_6^ℓ and the

space $\nabla E_3 = \{\nabla u, u \in E_3\}$, denoted $e_{H_0^1}$, is also computed using the L^2 orthogonal projection of ∇U_6^ℓ onto ∇E_3 .

In Tables 2 and 3, the convergence orders of e_{L^2} , $e_{H_0^1}$ and e_{λ_6} are reported. They are evaluated from the error ratio between two successive meshes that display very stable behaviour, detecting no oscillation. The displayed error rates are estimated between the two finest meshes.

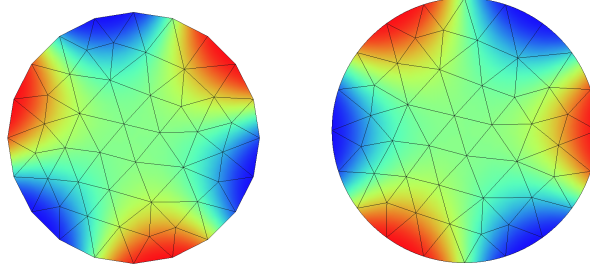


Figure 2: Display of the eigenfunction U_6 associated to the computed eigenvalue Λ_6 using \mathbb{P}^3 method on an affine mesh (left) and a quadratic mesh (right).

	e_{L^2}				$e_{H_0^1}$			
	\mathbb{P}^1	\mathbb{P}^2	\mathbb{P}^3	\mathbb{P}^4	\mathbb{P}^1	\mathbb{P}^2	\mathbb{P}^3	\mathbb{P}^4
Affine mesh ($r=1$)	2.01	2.48	2.48	2.48	1.00	1.51	1.50	1.50
Quadratic mesh ($r=2$)	2.01	3.07	4.5	4.47	1.00	2.01	3.5	3.49
Cubic mesh ($r=3$)	2.01	2.47	3.48	4.49	0.99	1.49	2.48	3.49

Table 2: Convergence order of the eigenfunctions errors in L^2 and H_0^1 norms (Figures in red represent a loss in the convergence rate).

The H_0^1 error convergence rate in Table 2 is equal to $\min\{k, r + 1/2\}$, for the most part: on an affine mesh, the order of $e_{H_0^1}$ is equal to 1.5, for all \mathbb{P}^k method with $k \geq 2$, as expected. On the quadratic mesh, similarly to the result in Table 1, the quadratic mesh acts like a cubic mesh: the error rate is equal to 3.5 instead of 2.5 for a \mathbb{P}^4 method, as if r is equal to 3. However, one needs to point out that, with a \mathbb{P}^3 method, the order is equal to 3.5 surpassing the expected value equal to 3. A possible explanation for this phenomenon is that the eigenspace E_3 associated to λ_6 is equal to the space of harmonic polynomials of degree 3 on the disk, as stated before. Moreover, the finite element approximation space \mathbb{V}_h is also made of polynomials on most of the domain (all the elements that do not have an edge on the boundary, i.e. $\Omega \setminus B_h^\ell$ where B_h^ℓ is defined in Corollary 5.1). This large vicinity between E_3 and \mathbb{V}_h may be a possible cause for the super convergence observed here. Lastly, on the cubic mesh, for a \mathbb{P}^4 method the rate of $e_{H_0^1}$ is equal to 3.5, as anticipated. However, oddly, for a \mathbb{P}^2 and \mathbb{P}^3 method, a loss in the order of convergence of $e_{H_0^1}$ is depicted and highlighted in red. Instead of having a convergence rate equal to 2 (resp. 3) for a \mathbb{P}^2 (resp. \mathbb{P}^3) method we obtained 1.5 (resp. 2.49). This is discussed in more details in the following paragraph.

The L^2 error convergence rates are displayed in Table 2, where a super convergence is quickly noticed: in the affine case ($r = 1$), the convergence rate of e_{L^2} is equal to 2.5 instead of 1.5 for a \mathbb{P}^k method with $k \geq 2$. As discussed previously, a super convergence is observed on the quadratic mesh: the quadratic mesh acts like the cubic mesh with $r = 3$. However, the convergence order depicted in Table 2 is equal to 4.5 surpassing the expected order of 3.5 for a \mathbb{P}^3 and \mathbb{P}^4 method. In

the cubic case, the convergence rate is equal to 4.5 instead of 3.5 for a \mathbb{P}^4 method. A plausible reason for this super convergence on all curved meshes of order $r = 1, 2, 3$ is that the L^2 estimate (5.2) is not optimal. In the light of these numerical results, we can formulate the following conjecture which may be a more accurate version of the obtained estimate (5.2):

$$e_{L^2} \leq c_{\lambda_i}(h^{k+1} + h^{r+1}). \quad (6.1)$$

We obtained a similar error estimate in the L^2 norm in [9] for a Ventcel problem with source terms. However we have not been able to prove this estimate (6.1). One has to point out that even with the estimate (6.1) a super convergence is still observed in the following cases: on affine mesh with a \mathbb{P}^k method with $k \geq 2$, the rate of e_{L^2} is equal to 2.5 instead of $2 = r + 1$. Additionally, on quadratic meshes with a \mathbb{P}^3 and \mathbb{P}^4 method, the order of e_{L^2} is equal to 4.5 instead of $4 = r + 1$. Similarly, on cubic meshes with a \mathbb{P}^4 method, the error order is equal to 4.5 instead of $4 = r + 1$. As stated in the case of the H_0^1 error, the large similarity between the eigenspace E_3 associated to λ_6 and the finite element space \mathbb{V}_h may be a possible cause for this super convergence.

One needs to stress that for these both errors $e_{H_0^1}$ and e_{L^2} , similarly to the results in Table 1, a loss in the convergence rate is detected on a cubic mesh with a \mathbb{P}^2 and \mathbb{P}^3 method. This convergence default of $-1/2$ is already discussed for the H_0^1 error in the previous paragraph, and it is also observed in the case of the L^2 error: the convergence rate of e_{L^2} is equal to 2.5 for the \mathbb{P}^2 method instead of 3. So far we are not able to fully explain this convergence default on cubic meshes. Moreover as discussed in [9], we noticed that it is only related to "volume norms", since the numerical errors computed in $L^2(\Gamma)$ and $H^1(\Gamma)$ norms show the expected convergence rate. Numerical experiments we have led in this direction show that this lack of convergence is not related to the lift. This lack of convergence is associated with the interpolation error between a smooth function u and its finite element interpolant $\mathcal{I}u \in \mathbb{V}_h$, denoted $\|\mathcal{I}u - u\|_{H^1(\Omega_h^{(r)})}$. On the considered cubic meshes, this error behaves like $O(h^{k-1/2})$ instead of $O(h^k)$ for $k \geq 2$. While conducting some experiments, we noticed that this interpolation error is highly sensitive to the position of the central node in cubic elements without being able so far to overcome this issue.

Mesh type	e_{λ_6}			
	\mathbb{P}^1	\mathbb{P}^2	\mathbb{P}^3	\mathbb{P}^4
Affine ($r=1$)	2.00	2.00	2.00	2.00
Quadratic ($r=2$)	2.00	4.01	4.01	3.99
Cubic ($r=3$)	2.00	3.27	3.89	4.00

Table 3: Convergence order of $e_{\lambda_6} = |\lambda_6 - \Lambda_6|$ (Figures in red represent a loss in the convergence rate).

The convergence rates of e_{λ_6} observed in Table 3 are analogous to the results of Table 1. As anticipated, the quadratic mesh ($r = 2$) behaves as if r is taken equal to 3: the convergence rate is equal to 4 instead of 3, for all \mathbb{P}^k method with $k \geq 2$. A loss in the convergence rate is highlighted in red in Table 3 and in Table 1, in the cubic case ($r = 3$) for a \mathbb{P}^2 method. Indeed, in the same case, the H_0^1 order of convergence for the associated eigenfunction in Table 2 is equal to 1.5 instead of 2 (see Table 2). This seems to imply an order of convergence of $2 \times 1.5 = 3$ instead of $2 \times 2 = 4$ for the eigenvalues.

6.2 A 3D case: error estimates on the unit ball

To conclude these numerical experiments, the system (1.1) is now considered on the unit ball $B(O, 1) \subset \mathbb{R}^3$. The ball is discretized using meshes of order $r = 1, \dots, 3$, which are depicted in

Figure 3 for affine and quadratic meshes. A convergence analysis is performed on the 10th eigenvalue λ_{10} of multiplicity 7. Since on the unit ball, the eigenfunctions are the harmonic polynomial, the corresponding eigenspace E_3 to λ_{10} is equal to the space of harmonic polynomials of degree 3.

For each mesh order r and finite element degree k , we compute the 12 first eigenvalues on a series of five successively refined meshes: it has been necessary to consider these five meshes in order to obtain a reliable estimation of the convergence rates (considering a 6th mesh however would have been unaffordable in terms of computational efforts). Each mesh counts $20 \times 2^{n-1}$ edges on the equator circle, for $n = 1, \dots, 5$. The most refined mesh has approximately $2,4 \times 10^6$ tetrahedra and the associated \mathbb{P}^3 finite element method counts 11×10^6 degrees of freedom. Consequently the matricial system of the spectral problem, which needs to be solved, has a size 11×10^6 with a rather large stencil. As a result, in the 3D case, the computations are much more demanding, both in terms of CPU time and of memory consumption. The use of MUMPS, as we did in the 2D case, is no longer an option due to memory limitation. The inversion of the linear system is done using the conjugate gradient method with a Jacobi preconditioner. With this strategy, 8 iterations of ARPACK were in general required to reach convergence (with a tolerance threshold of $1E - 14$ as stated in this section's introduction): each iteration of ARPACK required roughly 130 linear system inversions, each of which involving 2 000 iterations of the preconditioned CG algorithm. To handle these computations, we resorted to the UPPA research computer cluster PYRENE⁶. Using shared memory parallelism on a single CPU with 32 cores and 2 000 Mb of memory, each case required between 10 to 30 hours of computations.

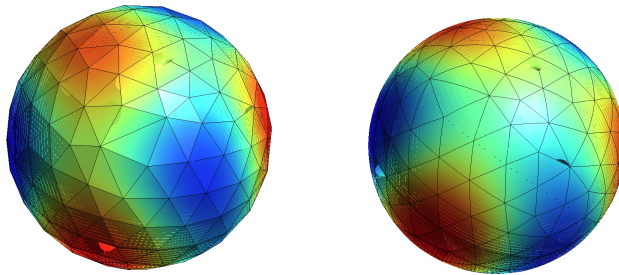


Figure 3: Display of the eigenfunction associated with the eigenvalue Λ_{10} using \mathbb{P}^2 finite element on an affine mesh (left) and a quadratic mesh (right).

Denote Λ_{10} a numerical eigenvalue approximating λ_{10} with U_{10} as its associated computed eigenfunction. In each case, the following numerical errors are computed on a series of refined meshes,

$$e_{L^2} := \inf \{ \|U_{10}^\ell - u\|_{L^2(\Omega)}, u \in E_3 \}, \quad e_{H_0^1} := \inf \{ \|\nabla(U_{10}^\ell - u)\|_{L^2(\Omega)}, u \in E_3 \},$$

and $e_{\lambda_{10}} := |\lambda_{10} - \Lambda_{10}|.$

Similarly to the disk case, orthogonal projections onto E_3 are used in order to compute the L^2 (resp. H_0^1) distance between U_{10}^ℓ and the eigenspace E_3 , denoted e_{L^2} (resp. $e_{H_0^1}$).

⁶PYRENE Mesocentre de Calcul Intensif Aquitain, <https://git.univ-pau.fr/num-as/pyrene-cluster>

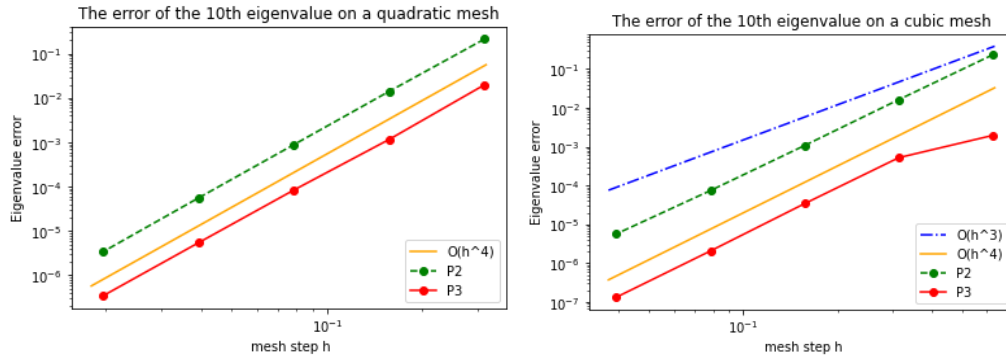


Figure 4: Display of the convergence rate of $e_{\lambda_{10}} = |\lambda_{10} - \Lambda_{10}|$ using \mathbb{P}^2 and \mathbb{P}^3 finite element on a quadratic mesh (left) and a cubic mesh (right).

In Figure 4, is displayed a log–log graph of the error $e_{\lambda_{10}}$ with respect to the mesh step, on a quadratic mesh (right) and a cubic mesh (left). In the quadratic case, as in the two dimensional experiments, the error is in $O(h^4)$ whereas $O(h^3)$ was expected from the theory. The same super convergence of quadratic meshes is present as in the 2D case: it is very interesting to underline this behaviour of the quadratic meshes, which brought a $O(h^4)$ geometric error also in three dimensions. In the cubic case, when using a \mathbb{P}^2 method, the convergence rate of $e_{\lambda_{10}}$ starts around 4 tending to 3, in hopes of following the loss in the convergence rate observed in the 2D case. Note that for the 10th eigenvalue, its asymptotic regime is quite harder to capture than the first ones. For an eigenvalue λ_j with lower rank $j < 10$, the convergence rate goes faster to 3, strengthening the hypothesis of a convergence loss in this case, as observed in the 2D case. Finally, when using a \mathbb{P}^3 method on a cubic mesh the error $e_{\lambda_{10}}$ seems to be in $O(h^4)$, following Inequality (5.1).

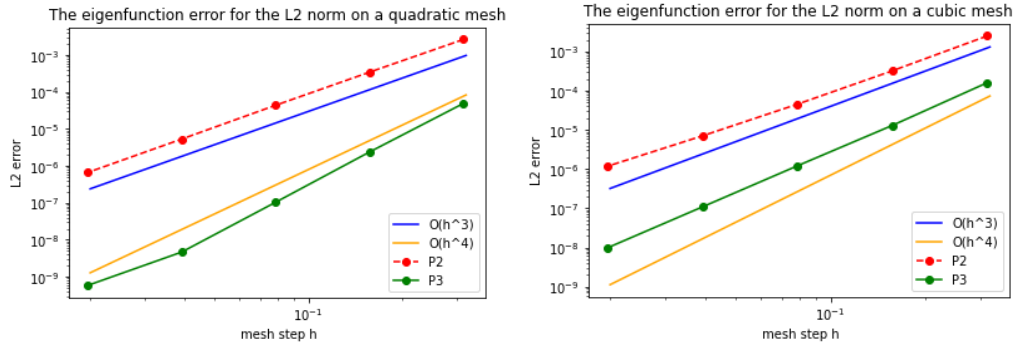


Figure 5: Display of the convergence rate of e_{L^2} using \mathbb{P}^2 and \mathbb{P}^3 finite element on a quadratic mesh (left) and a cubic mesh (right).

In Figure 5, is displayed a log–log graph of the L^2 error e_{L^2} with respect to the mesh step, on a quadratic mesh (right) and a cubic mesh (left). On the quadratic mesh, for a \mathbb{P}^2 method, the order of e_{L^2} is equal to 3, as expected. However, for a method of degree $k = 3$, the error order seems to be slightly more than 4 for the first 4 meshes. Though the convergence rate decreases on the last point, this seems to confirm that super convergence for quadratic meshes also holds on the eigenfunctions in 3D. In the cubic case with a \mathbb{P}^2 (resp. \mathbb{P}^3) method, the graph of e_{L^2} seems to have a slope approximately equal to 2.5 (resp. 3.5). The same loss in convergence as in the 2D case

is observed, see Table 2: this convergence default of $-1/2$ has been formerly discussed in the 2D case.

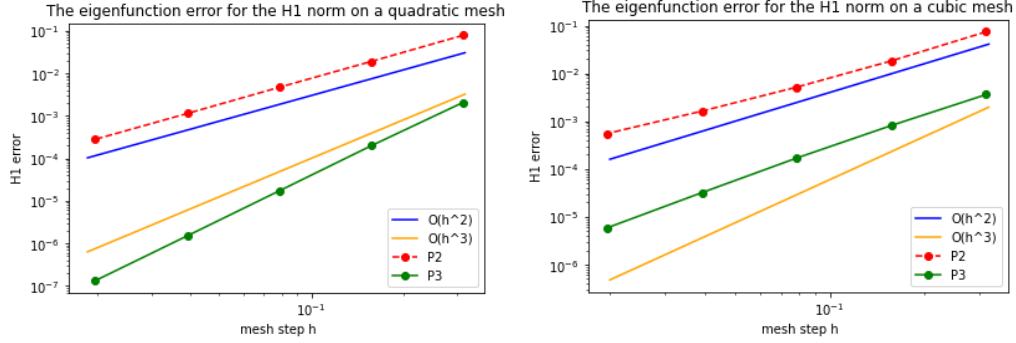


Figure 6: Display of the convergence rate of $e_{H_0^1}$ using \mathbb{P}^2 and \mathbb{P}^3 finite element on a quadratic mesh (left) and a cubic mesh (right).

Concerning the H_0^1 error, the results obtained in Figure 6 agree with the rates obtained on the disk. The convergence order is equal to 2 on the quadratic mesh with a finite element degree $k = 2$. With a \mathbb{P}^3 method, the graph of $e_{H_0^1}$ seems to have a slope around 3.5 higher than the awaited value of 3. As for the cubic mesh, the loss in the convergence rate of $e_{H_0^1}$ was already observed and discussed in the case of the disk: for a \mathbb{P}^2 (resp. \mathbb{P}^3) method, one can assess that the order of $e_{H_0^1}$ is slightly less than 2 (resp. 3), similarly to Table 2.

A Mesh construction

A.1 Affine mesh $\mathcal{T}_h^{(1)}$

Let $\mathcal{T}_h^{(1)}$ be a polyhedral mesh of Ω made of simplices of dimension d (triangles or tetrahedra), it is chosen as quasi-uniform and henceforth shape-regular (see [7, definition 4.4.13]). Define the mesh size $h := \max \{ \text{diam}(T); T \in \mathcal{T}_h^{(1)} \}$, where $\text{diam}(T)$ is the diameter of T . The mesh domain is denoted by $\Omega_h^{(1)} := \cup_{T \in \mathcal{T}_h^{(1)}} T$. Its boundary denoted by $\Gamma_h^{(1)} := \partial\Omega_h^{(1)}$ is composed of $(d - 1)$ -dimensional simplices that form a mesh of $\Gamma = \partial\Omega$. The vertices of $\Gamma_h^{(1)}$ are assumed to lie on Γ . For $T \in \mathcal{T}_h^{(1)}$, we define an affine function that maps the reference element \hat{T} onto T , $F_T : \hat{T} \rightarrow T := F_T(\hat{T})$. For more details, see [12, page 239].

A.2 Exact mesh $\mathcal{T}_h^{(e)}$

In the 1970's, many authors gave an explicit construction of an exact triangulation (see [32, 29]). In this subsection, is recalled the definition of an exact mesh given in [20, §4], [19, §3.2] and [10, §2]. The present definition of an exact transformation $F_T^{(e)}$ combines the definitions found in [29, 32] with the orthogonal projection b as used in [16].

Let us first point out that for a sufficiently small mesh size h , a mesh element T cannot have $d + 1$ vertices on the boundary Γ , due to the quasi uniform assumption imposed on the mesh $\mathcal{T}_h^{(1)}$.

Definition A.1. Let $T \in \mathcal{T}_h^{(1)}$ be a non-internal element (having at least 2 vertices on the boundary). Denote $v_i = F_T(\hat{v}_i)$ as its vertices, where \hat{v}_i are the vertices of \hat{T} . We define $\varepsilon_i = 1$ if $v_i \in \Gamma$ and $\varepsilon_i = 0$ otherwise. To $\hat{x} \in \hat{T}$ is associated its barycentric coordinates λ_i associated to the vertices \hat{v}_i of \hat{T} and $\lambda^*(\hat{x}) := \sum_{i=1}^{d+1} \varepsilon_i \lambda_i$ (shortly denoted by λ^*). Finally, we define $\hat{\sigma} := \left\{ \hat{x} \in \hat{T}; \lambda^*(\hat{x}) = 0 \right\}$ and the function $\hat{y} := \frac{1}{\lambda^*} \sum_{i=1}^{d+1} \varepsilon_i \lambda_i \hat{v}_i \in \hat{T}$, which is well defined on $\hat{T} \setminus \hat{\sigma}$.

Consider a non-internal mesh element $T \in \mathcal{T}_h^{(1)}$ and the affine transformation F_T . In the two dimensional case, $F_T(\hat{\sigma})$ will consist of the only vertex of T that is not on the boundary Γ . In the three dimensional case, the tetrahedral T either has 2 or 3 vertices on the boundary. In the first case, $F_T(\hat{\sigma})$ is the edge of T joining its two internal vertices. In the second case, $F_T(\hat{\sigma})$ is the only internal vertex of T .

Definition A.2. We denote $\mathcal{T}_h^{(e)}$ the mesh consisting of all exact elements $T^{(e)} = F_T^{(e)}(\hat{T})$, where $F_T^{(e)} = F_T$ for all internal elements, as for the case of non-internal elements $F_T^{(e)}$ is given by,

$$F_T^{(e)} : \begin{array}{l} \hat{T} \longrightarrow T^{(e)} := F_T^{(e)}(\hat{T}) \\ \hat{x} \longmapsto F_T^{(e)}(\hat{x}) := \begin{cases} x & \text{if } \hat{x} \in \hat{\sigma}, \\ x + (\lambda^*)^{r+2}(b(y) - y) & \text{if } \hat{x} \in \hat{T} \setminus \hat{\sigma}, \end{cases} \end{array} \quad (\text{A.1})$$

with $x = F_T(\hat{x})$ and $y = F_T(\hat{y})$. It has been proveen in [20] that $F_T^{(e)}$ is a \mathcal{C}^1 -diffeomorphism and C^{r+1} regular on \hat{T} .

B The lift transformation

We recall that the idea of lifting a function from the discrete domain onto the continuous one was already treated and discussed in many articles dating back to the 1970's, like [30, 32, 29, 5]. The key ingredient is a well defined lift transformation going from the mesh domain onto the physical domain Ω .

We recall the *lift* transformation $G_h^{(r)}$, which was defined in [9, §4]. Following the notations given in Definition A.1, the transformation $G_h^{(r)}$, is given piecewise for all $T^{(r)} \in \mathcal{T}_h^{(r)}$ by,

$$G_h^{(r)}|_{T^{(r)}} := F_{T^{(r)}}^{(e)} \circ (F_T^{(r)})^{-1}, \quad F_{T^{(r)}}^{(e)}(\hat{x}) := \begin{cases} x & \text{if } \hat{x} \in \hat{\sigma} \\ x + (\lambda^*)^{r+2}(b(y) - y) & \text{if } \hat{x} \in \hat{T} \setminus \hat{\sigma}, \end{cases} \quad (\text{B.1})$$

with $x := F_T^{(r)}(\hat{x})$ and $y := F_T^{(r)}(\hat{y})$, where $F_T^{(r)}$ is the \mathbb{P}^r -Lagrange interpolant of $F_T^{(e)}$ defined Section 3. By definition, we have $G_h^{(r)}|_{T^{(r)}} = id|_{T^{(r)}}$, for any internal mesh element $T^{(r)} \in \mathcal{T}_h^{(r)}$.

C Proof of inequality (5.15)

Keeping in mind the definition of $\Pi_h : H^1(\Omega, \Gamma) \rightarrow \mathbb{V}_h$ as the Riesz projection in Definition 5.1, we want to prove the estimate (5.15), given by,

$$\|u - \Pi_h u\|_{m_h^\ell} \leq ch^{k+1}.$$

To prove this estimate, we need to recall the definition of an interpolant, which can be found in [9]. Keeping in mind that \mathbb{V}_h denotes the \mathbb{P}^k -Lagrangian finite element space, let the \mathbb{P}^r -Lagrangian interpolation operator be denoted by $\mathcal{I}^{(r)} : \mathcal{C}^0(\Omega_h) \rightarrow \mathbb{V}_h$.

The lifted finite element space is given by, $\mathbb{V}_h^\ell := \{v_h^\ell, v_h \in \mathbb{V}_h\}$, with its lifted finite element interpolation operator \mathcal{I}^ℓ defined as follows,

$$\begin{aligned} \mathcal{I}^\ell : \mathcal{C}^0(\Omega) &\longrightarrow \mathbb{V}_h^\ell \\ v &\longmapsto \mathcal{I}^\ell(v) := (\mathcal{I}^{(r)}(v \circ G_h^{(r)}))^\ell. \end{aligned}$$

Notice that, since Ω is an open subset of \mathbb{R}^2 or \mathbb{R}^3 , then we have the following Sobolev injection $\mathbb{H}^{k+1}(\Omega) \hookrightarrow \mathcal{C}^0(\Omega)$. Thus, any function $w \in \mathbb{H}^{k+1}(\Omega)$ may be associated to an interpolation element $\mathcal{I}^\ell(w) \in \mathbb{V}_h^\ell$.

We recall its associated interpolation inequality, which is proved in [9, Proposition 6].

Proposition C.1. *Let $v \in \mathbb{H}^{k+1}(\Omega, \Gamma)$ and $2 \leq m \leq k+1$. The operator \mathcal{I}^ℓ satisfies the interpolation inequality with a constant $c > 0$ as follows,*

$$\|v - \mathcal{I}^\ell v\|_{L^2(\Omega, \Gamma)} + h\|v - \mathcal{I}^\ell v\|_{\mathbb{H}^1(\Omega, \Gamma)} \leq ch^m \|v\|_{\mathbb{H}^m(\Omega, \Gamma)}. \quad (\text{C.1})$$

Secondly, we define the functional F_h on $\mathbb{H}^1(\Omega, \Gamma)$ as follow,

$$\begin{aligned} F_h : \mathbb{H}^1(\Omega, \Gamma) &\longrightarrow \mathbb{R} \\ v &\longmapsto F_h(v) = (a - a_h^\ell)(u - \Pi_h u, v), \end{aligned}$$

where a is the continuous bilinear forms defined on $[\mathbb{H}^1(\Omega, \Gamma)]^2$ in Section 2 and a_h^ℓ is the lift of the discrete bilinear form defined on $[\mathbb{V}_h^\ell]^2$ in Section 4. Notice that for $v \in \mathbb{V}_h^\ell$, $F_h(v) = a(u - \Pi_h u, v)$, by Definition 5.1 of Π_h .

In order to prove the inequality (5.15), we proceed by bounding F_h as follows in Lemma C.1, with the help of the inequality (C.1)

Lemma C.1. *Let $v \in \mathbb{H}^1(\Omega, \Gamma)$, there exists $c > 0$ such that,*

$$|F_h(v)| \leq ch^{k+r} \|v\|_{\mathbb{H}^1(\Omega, \Gamma)}. \quad (\text{C.2})$$

Proof. Denote $e := u - \Pi_h u$. Let $v \in \mathbb{H}^1(\Omega, \Gamma)$, using Inequality (5.7) we have,

$$\begin{aligned} |F_h(v)| &= |a - a_h^\ell|(e, v) \leq ch^r \|e\|_{\mathbb{H}^1(\Omega, \Gamma)} \|v\|_{\mathbb{H}^1(\Omega, \Gamma)} + ch^{r+1} \|e\|_{\mathbb{H}^1(\Omega, \Gamma)} \|v\|_{\mathbb{H}^1(\Omega, \Gamma)} \\ &\leq ch^r (\|e\|_{\mathbb{H}^1(\Omega, \Gamma)} + ch\|e\|_{\mathbb{H}^1(\Omega, \Gamma)}) \|v\|_{\mathbb{H}^1(\Omega, \Gamma)}. \end{aligned}$$

Then applying the \mathbb{H}^1 error inequality (5.14), we get,

$$|F_h(v)| \leq ch^r (h^k + h^{k+1}) \|v\|_{\mathbb{H}^1(\Omega, \Gamma)} \leq ch^{k+r} \|v\|_{\mathbb{H}^1(\Omega, \Gamma)}. \quad \square$$

Proof of Inequality (5.15). To prove estimate (5.15), we use an Aubin-Nitche argument. Since $e \in L^2(\Omega)$, then there exists a unique solution $z_e \in \mathbb{H}^2(\Omega, \Gamma)$ solution of the weak formulation (2.1) with source terms satisfying,

$$\|z_e\|_{\mathbb{H}^2(\Omega, \Gamma)} \leq c\|e\|_{L^2(\Omega)}. \quad (\text{C.3})$$

We have, using the continuity of the bilinear form a ,

$$\begin{aligned} \|u - \Pi_h u\|_{L^2(\Omega)}^2 &= \|e\|_{L^2(\Omega)}^2 = a(e, z_e) = a(e, z_e - \mathcal{I}^\ell z_e) + a(e, \mathcal{I}^\ell z_e) \\ &\leq c_{cont} \|e\|_{\mathbb{H}^1(\Omega, \Gamma)} \|z_e - \mathcal{I}^\ell z_e\|_{\mathbb{H}^1(\Omega, \Gamma)} + |F_h(\mathcal{I}^\ell z_e)|. \end{aligned}$$

We apply the inequalities (5.14), (C.1) for $z_e \in H^2(\Omega, \Gamma)$ and (C.2) since $\mathcal{I}^\ell z_e \in \mathbb{V}_h^\ell$, as follows,

$$\|u - \Pi_h u\|_{L^2(\Omega)}^2 \leq c(h^k)h \|z_e\|_{H^2(\Omega, \Gamma)} + ch^{k+r} \|z_e\|_{H^1(\Omega, \Gamma)} \leq ch^{k+1} \|z_e\|_{H^2(\Omega, \Gamma)}.$$

By applying (C.3) and dividing by $\|u - \Pi_h u\|_{L^2(\Omega)}$, we obtain,

$$\|u - \Pi_h u\|_{L^2(\Omega)} \leq ch^{k+1}.$$

By the equivalence between the norms the norms $\|\cdot\|_m = \|\cdot\|_{L^2(\Omega)}$ and $\|\cdot\|_{m_h^\ell}$ in Corollary 5.2, we obtain (5.15). □

References

- [1] G. Allaire. *Numerical analysis and optimization*. Numerical Mathematics and Scientific Computation. Oxford University Press, Oxford, 2007.
- [2] I. Babuška and J. E. Osborn. Estimates for the errors in eigenvalue and eigenvector approximation by Galerkin methods, with particular attention to the case of multiple eigenvalues. *SIAM J. Numer. Anal.*, 24(6):1249–1276, 1987.
- [3] I. Babuška and J. E. Osborn. Finite element–Galerkin approximation of the eigenvalues and eigenvectors of selfadjoint problems. *Math. Comp.*, 52(186):275–297, 1989.
- [4] U. Banerjee and J. E. Osborn. Estimation of the effect of numerical integration in finite element eigenvalue approximation. *Numer. Math.*, 56(8):735–762, 1990.
- [5] C. Bernardi. Optimal finite-element interpolation on curved domains. *SIAM J. Numer. Anal.*, 26(5):1212–1240, 1989.
- [6] A. Bonito, A. Demlow, and J. Owen. A priori error estimates for finite element approximations to eigenvalues and eigenfunctions of the Laplace-Beltrami operator. *SIAM J. Numer. Anal.*, 56(5):2963–2988, 2018.
- [7] S. C. Brenner and L. R. Scott. *The mathematical theory of finite element methods*, volume 15 of *Texts in Applied Mathematics*. Springer-Verlag, New York, second edition, 2002.
- [8] C. Carstensen and J. Gedicke. An oscillation-free adaptive FEM for symmetric eigenvalue problems. *Numer. Math.*, 118(3):401–427, 2011.
- [9] F. Caubet, J. Ghantous, and C. Pierre. Numerical analysis of a diffusion equation with ventcel boundary condition using curved meshes. (*Accepted at SINUM*), 2023.
- [10] F. Caubet, J. Ghantous, and C. Pierre. Numerical study of a diffusion equation with ventcel boundary condition using curved meshes. *Monografías Matemáticas García de Galdeano*, 2023.
- [11] P. G. Ciarlet. *The finite element method for elliptic problems*, volume 40 of *Classics in Applied Mathematics*. Society for Industrial and Applied Mathematics (SIAM), Philadelphia, PA, 2002. Reprint of the 1978 original [North-Holland, Amsterdam; MR0520174 (58 #25001)].
- [12] P. G. Ciarlet and P.-A. Raviart. Interpolation theory over curved elements, with applications to finite element methods. *Comput. Methods Appl. Mech. Engrg.*, 1:217–249, 1972.
- [13] C. Dapogny and P. Frey. Computation of the signed distance function to a discrete contour on adapted triangulation. *Calcolo*, 49(3):193–219, 2012.

- [14] A. Demlow. Higher-order finite element methods and pointwise error estimates for elliptic problems on surfaces. *SIAM J. Numer. Anal.*, 47(2):805–827, 2009.
- [15] A. Demlow and G. Dziuk. An adaptive finite element method for the Laplace-Beltrami operator on implicitly defined surfaces. *SIAM J. Numer. Anal.*, 45(1):421–442, 2007.
- [16] F. Dubois. Discrete vector potential representation of a divergence-free vector field in three-dimensional domains: numerical analysis of a model problem. *SIAM J. Numer. Anal.*, 27(5):1103–1141, 1990.
- [17] G. Dziuk. Finite elements for the Beltrami operator on arbitrary surfaces. In *Partial differential equations and calculus of variations*, volume 1357 of *Lecture Notes in Math.*, pages 142–155. Springer, Berlin, 1988.
- [18] G. Dziuk and C. M. Elliott. Finite element methods for surface PDEs. *Acta Numer.*, 22:289–396, 2013.
- [19] D. Edelmann. Isoparametric finite element analysis of a generalized Robin boundary value problem on curved domains. *SMAI J. Comput. Math.*, 7:57–73, 2021.
- [20] C. M. Elliott and T. Ranner. Finite element analysis for a coupled bulk-surface partial differential equation. *IMA J. Numer. Anal.*, 33(2):377–402, 2013.
- [21] A. Ern and J.-L. Guermond. *Theory and practice of finite elements*, volume 159 of *Applied Mathematical Sciences*. Springer-Verlag, New York, 2004.
- [22] D. Gallistl. An optimal adaptive FEM for eigenvalue clusters. *Numer. Math.*, 130(3):467–496, 2015.
- [23] S. Giani and I. G. Graham. A convergent adaptive method for elliptic eigenvalue problems. *SIAM J. Numer. Anal.*, 47(2):1067–1091, 2009.
- [24] D. Gilbarg and N. S. Trudinger. *Elliptic partial differential equations of second order*. Classics in Mathematics. Springer-Verlag, Berlin, 2001. Reprint of the 1998 edition.
- [25] G. R. Goldstein. Derivation and physical interpretation of general boundary conditions. *Adv. Differential Equations*, 11(4):457–480, 2006.
- [26] A. Henrot and M. Pierre. *Variation et optimisation de formes: une analyse géométrique*, volume 48. Springer Science & Business Media, 2006.
- [27] T. Kashiwabara, C. M. Colciago, L. Dedè, and A. Quarteroni. Well-posedness, regularity, and convergence analysis of the finite element approximation of a generalized Robin boundary value problem. *SIAM J. Numer. Anal.*, 53(1):105–126, 2015.
- [28] A. V. Knyazev and J. E. Osborn. New a priori FEM error estimates for eigenvalues. *SIAM J. Numer. Anal.*, 43(6):2647–2667, 2006.
- [29] M. Lenoir. Optimal isoparametric finite elements and error estimates for domains involving curved boundaries. *SIAM J. Numer. Anal.*, 23(3):562–580, 1986.
- [30] J.-C. Nédélec. Curved finite element methods for the solution of singular integral equations on surfaces in R^3 . *Comput. Methods Appl. Mech. Engrg.*, 8(1):61–80, 1976.
- [31] C. Pierre. The finite element library Cumin, curved meshes in numerical simulations. *repository: <https://plmlab.math.cnrs.fr/cpierre1/cumin>*, hal-0393713(v1), 2023.

- [32] R. Scott. Interpolated boundary conditions in the finite element method. *SIAM J. Numer. Anal.*, 12:404–427, 1975.
- [33] A. D. Ventcel. Semigroups of operators that correspond to a generalized differential operator of second order. *Dokl. Akad. Nauk SSSR (N.S.)*, 111:269–272, 1956.
- [34] A. D. Ventcel. On boundary conditions for multi-dimensional diffusion processes. *Theor. Probability Appl.*, 4:164–177, 1959.